0270-6474/83/0301-0203$02.00/0

The Journal of Neuroscience
Vol. 3, No. 1, pp. 203-224
January 1983

INTRINSIC ORGANIZATION OF THE CAT'S MEDIAL GENICULATE BODY IDENTIFIED BY PROJECTIONS TO BINAURAL RESPONSE-SPECIFIC BANDS IN THE PRIMARY AUDITORY CORTEX[1]

JOHN C. MIDDLEBROOKS[2] AND JOHN M. ZOOK

Coleman Memorial Laboratory and Neuroscience Graduate Program, University of California, San Francisco, California 94143

Received May 3, 1982; Revised August 3, 1982; Accepted August 3, 1982

Abstract

The area of the cat's primary auditory cortex (AI) within which high frequency sounds are represented can be subdivided using functional criteria. Within each subdivision, or "binaural interaction band," all recorded neurons display similar responses to binaural stimulation. The current study distinguishes the thalamic sources of input to these subdivisions of AI and characterizes the topography within the thalamic projection to each class of bands. The borders of binaural bands in AI were mapped using microelectrode recording with diotic tonal stimulation, then injections of one to three retrograde tracers were introduced into identified bands. Within the ventral division (V) of the medial geniculate body (the major thalamic souce of input to AI), the neuronal populations that projected to different classes of binaural bands were strictly segregated from each other. This segregation of class-specific thalamic sources constitutes a laminar organization within an axis of V that is orthogonal to the previously described tonotopic organization.

Excitatory/excitatory (EE) binaural neurons in AI were found to be segregated from excitatory/inhibitory (EI) neurons in alternating "bands." We consistently identified: (*1*) a ventral pair of rostrocaudally continuous EI and EE bands, (*2*) a middle area within which the pattern of binaural subdivisions was more variable and within which bands often were discontinuous rostrocaudally, and (*3*) a dorsal zone (DZ) within which the responses of neurons differed in binaural properties and in frequency specificity from the response patterns that were characteristic of neurons elsewhere in AI. Each EI band apparently derived input that converged from three thickened laminae of cells in V that were oriented approximately horizontally. The most ventral of these laminae encompassed the ovoidal part of V (Vo), suggesting that EI bands are the only recipients in AI of a projection from Vo. All of the EE bands and DZ derived their input from a single continuous structure which included the dorsal two-thirds of the rostral pole of V and a horizontal lamina interposed between the two dorsalmost EI-projecting laminae. Restricted portions of the complex EE-projecting structure in V projected preferentially to particular EE subdivisions of AI. The V-to-AI thalamocortical topography exhibited a high degree of convergence and divergence within the projections to each cortical binaural band and within the projections to each class of bands.

These observations indicate that the high frequency representation in AI and its principal thalamic source of input, the ventral division of the medial geniculate body, may be thought of as assemblies of spatially discrete, functionally distinguishable subunits. The significance of this intrinsic organization is discussed in regard to the requirements for analysis of sound stimuli.

The primary auditory cortex (AI) of the cat contains functionally distinguishable topographical subdivisions. Within each subdivision, all recorded neurons display similar responses to binaural stimulation (Imig and Ad-

[1] This study formed part of a doctoral dissertation for the Neuroscience Graduate Program at the University of California at San Francisco (Middlebrooks, 1982). Nuclear Yellow was supplied by Dr. Heinz Loewe. Dr. Allan Basbaum encouraged us to use fluorescent dyes as retrograde tracers and generously extended to us the use of his fluorescence microscope. The manuscript benefitted from critical readings by Drs. E. I. Knudsen, M. M. Merzenich, and M. P. Stryker. We are indebted to Dr. Michael M. Merzenich for his support throughout the course of this study and for his valuable contributions during the preparation of the manuscript. This study was supported by the Coleman Memorial Fund and National Institutes of Health Grant NS 10414 (to M. M. Merzenich).

[2] To whom correspondence should be addressed at his current address: Department of Neurobiology, Stanford University School of Medicine, Stanford, CA 94305.

rian, 1977; Imig and Brugge, 1978; Middlebrooks et al., 1980; Imig and Reale, 1981). Neurons which respond optimally to stimulation of both ears or respond to monaural stimulation of each ear ("excitatory/excitatory;" EE) occupy radially organized modules which are segregated from modules of neurons which are excited by stimulation of the contralateral ear and inhibited by ipsilateral stimulation ("excitatory/inhibitory" EI). These "binaural interaction bands" are elongated rostrocaudally, parallel to the axis of representation of the cochlear sensory epithelium (i.e., roughly orthogonal to the isofrequency contours of AI).

The rostrocaudally elongated shape of binaural interaction bands in AI has been described in several reports (Imig and Adrian, 1977; Imig and Brugge, 1978; Middlebrooks et al., 1980; Imig and Reale, 1981). However, the dimensions of bands apparently are highly variable among different cats. Details of the organization of the bands, such as their numbers, dimensions, and neuronal response characteristics beyond the basic EE/EI distinction, have not been determined, nor have the sources of input to different bands been defined. What is the meaning of the apparent variability in the banding pattern in different cats? Are binaural bands functional subunits which contribute in ensemble to a unified product of AI, or are they largely independent parallel processing regions within AI? By the criteria enunciated by Rose and Woolsey (Rose, 1949; Rose and Woolsey, 1949), a cortical field is defined by: (*1*) characteristic neural response properties, (*2*) distinguishable cytoarchitectonic features, and (*3*) field-specific input and output connections. How are these criteria met by AI *and by its binaural bands*? These studies have been undertaken to begin to address these questions.

Recent studies of the distribution of thalamic input to AI have characterized the basic pattern of projection from isofrequency laminae in the ventral division (V) of the medial geniculate body (MGB) to isofrequency contours in AI (Colwell, 1977; Colwell and Merzenich, 1975, 1982; Andersen et al., 1980a; Merzenich et al., 1982). Moderately sized injections of retrograde tracers centered within AI and spreading over only a fraction of its mediolateral extent resulted in retrograde labeling of *entire* isofrequency laminae in V, regardless of the position of the injection along the length of an isofrequency contour. Smaller injections of retrograde tracer introduced at sites of representation of high frequencies sometimes resulted in multiple discrete patches of labeled neurons located within isofrequency laminae in V. Those results suggested that a single locus in this principal thalamic input source to AI sends divergent projections to repeating subunits distributed along an isofrequency contour in AI and, conversely, that a narrow zone within an isofrequency contour can receive convergent projections from sources distributed across an entire isofrequency lamina. Merzenich et al. (1982) speculated that the discontinuous patches within an isofrequency lamina in V might be thalamic subunits that provide input to given binaural bands. Does each band (or class of bands) receive its input from a band-specific (or class-specific) neuronal population? Does the functionally defined intrinsic organization of AI reflect in some way an analogous intrinsic organization of the thalamus?

These questions have been addressed in a series of experiments which employed a combination of physiological and anatomical tracing techniques. The boundaries of binaural bands and the tonotopic organization within bands were defined by mapping AI in detail with microelectrodes while presenting diotic tonal stimuli. Subsequently, injections of one to three retrograde tracers were introduced into AI with reference to these functional maps. Two binaural bands in the ventral aspect of AI were identified consistently in each mapped hemisphere. The arrays of cells in the MGB that project to these repeatedly encountered EE and EI bands were found to be largely segregated from each other within an apparently functionally subdivisible ventral division of the MGB. These complex neuronal arrays were remarkably constant in form among different individual cats. Injections introduced into EE and EI subdivisions located farther dorsal in AI demonstrated that bands that are of the same binaural class derive input from common thalamic sources. These results lead to a new view of the functional organization of the MGB and AI.

A preliminary report of these experiments has been presented elsewhere (Middlebrooks and Zook, 1981).

Materials and Methods

In each of these experiments, a sector of AI was mapped with microelectrodes, then retrograde tracers were introduced into functionally identified binaural bands. Attention was focused on the segment of AI in which frequencies greater than 5 kHz are represented. Within this higher frequency region of AI, binaural interaction bands are best defined, and injections of retrograde tracers previously have been shown to produce discontinuous patterns of label in the auditory thalamus (Colwell, 1977; Colwell and Merzenich, 1975, 1982; Andersen et al., 1980a; Merzenich et al., 1982).

Functional mapping

The results presented here are based on experiments using 38 adult cats selected for normal appearing external ears. Barbiturate anesthesia was used to maintain an areflexic state. The cortex was exposed and protected with a pool of silicone oil. The activity of single units and of small clusters of units was recorded in microelectrode penetrations oriented approximately normal to the cortical surface. The locations of penetrations were marked on a magnified photograph of the cortical surface, using the surface vasculature for positional reference. Best frequencies and binaural response characteristics were defined in the middle cortical layers in which reliable responses can be recorded in the barbiturate-anesthetized preparation.

Sound stimuli consisted of tone bursts shaped with 5-msec rise/fall times. Tones were generated using headphones (Beyer) that were coupled to hollow ear bars sealed into the ear canals. The intensities of stimuli presented to the two ears were controlled independently with decade attenuators. Contralateral monaural tone bursts were used as search stimuli. When no response could be evoked with monaural stimuli, binaural tone bursts of equal intensity were used. The characteristic frequencies (CFs) of units and of unit clusters were determined by finding the frequency of the lowest intensity tone burst with which neural responses could be

evoked. Once CF was defined, the binaural response class was determined using CF tone pips. Units were assigned to one of two binaural classes by observing the effect of stimulation of the ipsilateral ear on the threshold for contralateral stimulation. Electrode penetrations in which ipsilateral stimulation added to or facilitated the responses of units to contralateral stimulation or in which units responded to monaural stimulation of each ear were classified as excitatory/excitatory (EE). Penetrations in which ipsilateral stimulation inhibited contralaterally evoked unit responses were classified as excitatory/inhibitory (EI). In some penetrations that were classified as "EE," units were not driven by stimulation of either ear alone at any stimulus level, although they responded with low thresholds to binaural stimulation. In the vast majority of radial electrode penetrations in AI, units recorded along the entire length of the penetration had CFs falling within a narrow range and were of the same binaural class (see Merzenich et al., 1975; Imig and Adrian, 1977; Middlebrooks et al., 1980). Thus, each penetration could be represented with respect to these simple parameters by a single point on a map of the cortical surface.

Significant variation was observed in response properties within each binaural class, such as differences in relative thresholds for the two ears, "aural dominance," "facilitation" versus "summation" in EE responses, etc. (see Imig and Adrian, 1977; Kitzes et al., 1980; Phillips and Irvine, 1981). A more quantitative characterization of responses probably would have enabled us to distinguish several subclasses. At the same time, the simple dichotomous classification scheme that was used provided a straightforward basis for identifying functional boundaries within AI. The relevance of this classification scheme to functional organization was substantiated by the consistent patterns of thalamocortical topography that were observed.

The recognition of constant features of binaural representation was facilitated by determining carefully the location of the border between AI and the second auditory field (AII), which lies ventral to AI. This border was defined in 21 cases. Recordings from AII near the AI/AII border are characterized by broad frequency tuning compared to the sharp tuning characteristics of recordings from AI (see Merzenich et al., 1975; Reale and Imig, 1980). While unit clusters in AI had clearly defined CFs, clusters in AII often responded to frequencies ranging over an octave at levels only 10 dB above the threshold for the best frequency. In occasional penetrations in which the distinction between characteristic AI and AII neural responses was in question, the effect on neural thresholds of reducing the rise time of the tone burst was tested. The resulting increase in spectral complexity commonly reduced the thresholds of unit clusters in AII by 10 to 20 dB, while it had no effect or even increased the threshold of units or clusters in AI. Using one or both of these criteria, the AI/AII border could be defined clearly. Given this boundary definition, specific binaural bands could be identified repeatedly.

Retrograde tracing

The microelectrode maps of each hemisphere were used to guide the placement of microinjections of retrograde tracers. Injections were positioned with reference to the boundaries of identified binaural bands at sites of known characteristic frequency. Injections were made through glass micropipettes (30- to 40-μm tips, beveled) sealed to a 1-μl syringe (Unimetrics). When care was taken to exclude all air bubbles from the micropipette and syringe, it was possible to make reliable mechanical injections with volumes in the range of tens of nanoliters. In some cases, horseradish peroxidase (HRP) was used as the only retrograde tracer. In other studies, multiple retrograde tracers were used to compare directly the sources of input to several binaural bands in the same preparation. Protocols for single and multiple tracer studies will be described separately.

Single tracer experiments. Horseradish peroxidase (Boehringer Mannheim, grade I) was injected as a 30% solution in distilled water. The injection pipette was advanced 1.0 mm radially into the cortex and was left in place for 5 min following the injection. Injection volumes were 30 or 50 nl. After the pipette was withdrawn, the cortex was covered with Gelfilm (The Upjohn Co.), the temporal muscle was sutured in place, and the scalp was closed. Local and systemic antibiotics were administered. Following a survival period of approximately 30 hr, cats were anesthetized deeply and were perfused transcardially with a wash of warmed 0.1 M phosphate buffer containing 4% sucrose followed by a fixative of 4% glutaraldehyde, buffered, containing 4% sucrose. Brains were blocked stereotaxically and stored cold in buffered 30% sucrose for 2 days.

The brains were frozen and sectioned on a sliding microtome at 50 μm in the Horsley-Clarke coronal plane. Sections were reacted for peroxidase activity using tetramethyl benzidine (TMB) as the chromagen (Mesulam, 1978). After the reaction, the sections were transferred to cold acetate buffer (pH 3.3), then mounted on subbed slides. In some cases, alternate sections were counterstained with neutral red. The air-dried slides were cleared in methyl salicylate, rinsed briefly in xylene, then coverslipped with Eukitt (Calibrated Instruments, Inc.). This coverslipping procedure avoided exposing the tissue to ethanol, which can cause fading of the TMB reaction product (Adams, 1980).

Multiple tracer experiments. In some experiments, fluorescent dyes also were used as retrograde tracers. Good results were obtained using Nuclear Yellow (NY; Bentivoglio et al., 1980b) and propidium iodide (PI; Sigma Chemical Co.; Kuypers et al., 1979), in conjunction with HRP, to trace simultaneously the projections to three sites in AI. The histological protocol that was used reflects a compromise among the particular requirements for each of the three tracers.

The fluorescent dyes were injected as suspensions in distilled water (1% and 0.75% for NY and PI, respectively) using micropipettes and a 1-μl syringe as described above. Effective injection sites for PI were more restricted than for equal volumes of NY or HRP. Therefore, injection volumes of 30, 30, and 100 nl typically were used for HRP, NY, and PI, respectively, to achieve effective injection sites of comparable size. Postinjection survival periods of 56 to 60 hr were used. This longer time was necessary for adequate visibility of transported PI. Transported NY was visible following survival times of

30 hr, but the transported label was seen more clearly with longer postinjection survivals. With a survival time of 56 to 60 hr, HRP-labeled cells were visualized readily in the thalamus; the injection site appeared more diffuse than after 30 hr.

A modified perfusion and sectioning protocol was necessary to retard the diffusion of NY (Bentivoglio et al., 1980a) while maintaining adequate HRP activity. Following an appropriate survival period, cats were anesthetized deeply and perfused transcardially with a wash of 0.1 M phosphate buffer containing 4% sucrose, followed by a fixative of buffered 2% paraformaldehyde containing 4% sucrose and 1.5% dimethyl sulfoxide (DMSO). The DMSO was added as a cryoprotectant in lieu of equilibration in 30% sucrose. Brains were blocked stereotaxically, then removed from the skull and frozen quickly in heptane on dry ice. Quick freezing was used to retard the formation of large ice crystals. Brains were sectioned on a cryostat at 32 μm in the Horsley-Clarke coronal plane, and the sections were mounted directly on two or three sets of subbed slides. One set of slides, for fluorescence photomicrography, was left unreacted and uncoverslipped. Another set of slides was reacted for peroxidase histochemistry (as described above), although in this case the reaction was carried out with the sections mounted on slides. This set of slides was cleared and coverslipped as described above.

The method of tissue preparation described here minimized the problem of migration of NY from labeled neurons into adjacent glial cells (Bentivoglio et al., 1980a, b). Nuclear Yellow label was concentrated within neurons and only faint NY label was seen in glia located in NY-labeled projection areas. It was necessary to straighten occasional wrinkled sections using a small brush and a drop of distilled water. In those sections, NY-labeled glial nuclei were seen more commonly and the intensity of label in neurons seemed to be somewhat reduced.

In the tissue reacted for HRP, the NY label survived remarkably well, although NY-labeled glia were abundant in that material and NY label appeared to be less concentrated within neurons. PI-labeled cells could not be identified in tissue reacted for HRP. The TMB reaction product in the tissue reacted on slides did not label neuronal processes as reliably as it did in tissue processed more conventionally, but the patterns of label within the thalamus and the average densities of labeled cells were comparable.

Data analysis

Histological materials were examined using transmitted light and fluorescence microscopy. A microprojector was used to draw the outlines of sections and the positions of HRP-labeled cells. Bright-field photomicrographs were made with a Nikon Multiphot macrophotography system. Fluorescence-labeled tissues were observed and photographed with a Zeiss Universal fluorescence microscope using excitation wavelengths of 360 nm for NY and 550 nm for PI. With these excitation wavelengths, NY-labeled cells appeared yellow against a blue background and PI-labeled cells were bright red against a dull red background. Fluorescence-labeled tissue was photographed on color positive film (Ektachrome 400, processed to yield a speed of ASA 800). The positions of fluorescence-labeled cells were marked on drawings of the section outlines by projecting the color film with a photographic enlarger and using blood vessels for alignment. Three-dimensional reconstructions of histological materials were made using a computer graphics system.

Interpretation of neuroanatomical experiments of this type is limited fundamentally by the ability to limit the size of the *effective* injection site. The *apparent* sizes of the injection sites were much greater than the area of cortex contributing to thalamic labeling and varied with the postinjection survival time, the fixation protocol (in the case of NY), and the sensitivity of the histochemical protocol (for HRP). Nevertheless, two lines of evidence indicate that injections could be restricted to single binaural interaction bands. (*1*) In cases where injections were centered within several hundred micrometers of the border of AI with AII, no labeled cells were seen in subunits of the MGB that are labeled by injections into AII (Andersen, 1979; Andersen et al., 1980a). (*2*) From the known tonotopic organization of AI (Merzenich et al., 1975) and the ventral division of the MGB (Colwell and Merzenich, 1975, 1982; Andersen et al., 1980a; the current results), one can calculate the relative magnification of the frequency representation in these two structures. Using this factor, the mediolateral thickness of the labeled isofrequency lamina in the ventral division (i.e., the amount of spread along the axis of tonotopic representation) can be related to the size of the effective injection site in AI. This calculation commonly yielded effective injection sites of the order of 0.5 to 1 mm in diameter.

Subdivision of the auditory thalamus. The nomenclature that we use for subdivision of the auditory thalamus follows the definitions of Morest (1964, 1965) and Jones and Powell (1971). The MGB has ventral (V), medial (M), and dorsal (D) divisions. The ventral division is the principal source of input to AI (e.g., Rose and Woolsey, 1949; Neff et al., 1956; Colwell, 1977; Colwell and Merzenich, 1975, 1982). It occupies the lateral and ventral aspect of the rostral two-thirds of the MGB and may be subdivided into lateral (Vl) and ovoidal (Vo) parts and a dorsal cap (Vdc).

These subdivisions were made apparent in our retrogradely labeled material by the variation within V of the pronounced laminar arrangement of perikarya and dendrites and of the orientation of the arrays of cells that project to the representation of a single frequency in AI. In Vl, located lateral and dorsal in V, the orientation of the apparent cellular laminae lies approximately parallel to the lateral margin of the MGB. In the dorsal aspect of Vl, the laminae turn medially to form Vdc which abuts the fibers of the acoustic radiation. In the ventral aspect of Vl, the cellular laminae curve medially into a transitional zone (Vt). The ovoidal part of V (Vo) lies ventral and is centered somewhat medial to Vl. Descriptions of Vo in Golgi material have emphasized the coiled appearance of the laminae, but in material in which the projection for a single frequency is labeled retrogradely, a single lamina oriented from dorsomedial to ventrolateral is more apparent (Colwell, 1977; Colwell and Merzenich, 1975, 1982; Andersen et al., 1980a; the current results).

The medial division consists of a population of large cells located among the fibers of the brachium of the inferior colliculus in the ventromedial aspect of the MGB. In our material, retrogradely labeled cells in M formed a cluster that lay medial to Vt, separated from V by bundles of fibers. In D, only the deep dorsal nucleus (Dd) was labeled retrogradely by injections in AI. This subdivision lies dorsal to M and medial and dorsal to V in the rostral two-thirds of the MGB. Laminae of retrogradely labeled cells in Dd were oriented from dorsolateral to ventromedial, while laminae in the dorsal part of Vl were oriented dorsomedial to ventrolateral. The fibers of the acoustic radiation delimit Dd and Vdc. The lateral part of the posterior thalamic group (POl) is continuous rostrally with Dd and lies medial to the fibers of the acoustic radiation. This is the subdivision of the posterior group which receives ascending input from the brachium of the inferior colliculus (Moore and Goldberg, 1963) and descending input from the auditory cortex (Jones and Powell, 1971).

Results

Sectors of AI were mapped in 24 hemispheres with detail sufficient to identify binaural bands and to position injections of retrograde tracers. Attention was focused on the segment of AI in which the upper three octaves of the audible frequency range are represented. Best frequencies and binaural response classes were defined at 32 to 120 cortical sites in each experiment. Injections of one to three retrograde tracers were introduced and projecting arrays to these restricted AI loci were reconstructed successfully in 17 of these cats. In every cat, units that exhibited similar responses to binaural stimulation occupied regions ("binaural interaction bands") that appeared to be elongated rostrocaudally. The border between AI and the second auditory field (AII) was defined in 19 binaural maps. In all of these cats, a band of excitatory/inhibitory (EI) units was identified at the ventral margin of AI; in every cat, it was bordered dorsally by a band of excitatory/excitatory (EE) units. In many of these cases, the dorsal part of AI also was explored. Along the dorsal margin of AI, a region was encountered within which responses differed in frequency specificity and binaural response (as described in more detail below) from those recorded elsewhere in the field. This region is referred to here as the dorsal zone (DZ). In the region of AI lying between DZ and the ventral binaural bands, the dimensions of alternating binaural "bands" were somewhat more variable; these bands often were not continuous rostrocaudally. Injections of retrograde tracers centered in the ventral EE and EI bands, in DZ, and in the middle binaural "bands" each resulted in characteristic arrays of retrogradely labeled neurons in the thalamus. Neurons in the ventral division (V) of the medial geniculate body (MGB) projecting to EI bands were segregated from those projecting to EE bands and to DZ (which was principally EE in binaural response character).

Microelectrode maps of AI are illustrated for four representative cases in Figure 1. The *symbols* indicate the sites of radial electrode penetrations and the classes of binaural responses that were recorded at each site. *Irregular vertical lines* indicate isofrequency contours that have been interpolated between recorded CFs and *diamonds* indicate the locations of some of the retrograde tracer injections that are discussed in later sections. In some penetrations, unusually broad frequency tuning was encountered (indicated in Fig. 1 with *triangles*). These penetrations fell within DZ, described below. Again, segments of the ventral EI and EE bands were identifiable in each illustrated map. The maps in Figure 1, *B*, *C*, and *D* extended across most of the width of AI, into DZ.

The composite AI projection pattern. In the case represented in Figure 2, an attempt was made to define the entire array of cells in the thalamus that projects to the representation of a single frequency in AI (see Colwell, 1977; Colwell and Merzenich, 1975, 1982; Andersen et al. 1980a). Five injections of horseradish peroxidase (HRP) were placed at even intervals along the length of the 17-kHz isofrequency contour. Labeled cells were found in all three major divisions of the MGB and in the lateral part of the posterior thalamic group (POl). As in all AI injection cases, labeled cells in the MGB were restricted to the rostral two-thirds of the structure. The major projection to AI was from V. There, labeled cells occupied a lamina which appeared in coronal section as a folded band caudally (Fig. 2*A*) and as a straight band rostrally (Fig. 2*C*). In the caudal and central areas of the array (see Fig. 2, *A* and *B*), the line of labeled cells passed from dorsolateral to ventromedial in the pars lateralis (Vl) through the transitional zone (Vt), then curved laterally to end in the pars ovoidea (Vo). At caudal levels (Fig. 2*A*), the line of labeled cells was interrupted between Vt and Vo; this unlabeled region appeared relatively free of neurons in adjacent Nissl-stained sections. At other levels (Fig. 2*B*), the pattern of labeled neurons was continuous through this region, making it difficult to define a Vt/Vo border. More rostral (Fig. 2*C*), the sheet of labeled cells in Vl moved progressively nearer the lateral margin of the nucleus. Here, the labeled neuronal sheet straightened and assumed a parasagittal orientation. A cluster of labeled cells in the medial division (M) lay across the brachium of the inferior colliculus from Vt (Fig. 2, *A* and *B*). At more rostral levels (Fig. 2, *B* and *C*), labeled cells occupied an often discontinuous sheet or column in the deep part of the dorsal division (Dd). The pattern of label in Dd varied considerably between cases, sometimes filling a narrow lamina or column and at other times appearing to be discontinuous, as in this case. The column of label in Dd continued rostrally into POl (Fig. 2*D*).

The arrays of labeled cells in Vl that resulted from injections centered on single isofrequency contours in AI correspond in position and orientation to the morphological laminae defined in cytoarchitectonic studies (see Morest, 1965). They will be referred to here as "isofrequency laminae." Our data for injections made at various locations along the cortical axis of representation of frequency are consistent with previous descriptions of topographic organization in the MGB (e.g., Colwell, 1977; Colwell and Merzenich, 1975, 1982; Andersen et al., 1980a). The most prominent effect of shifts of injection sites along the tonotopic (rostrocaudal) axis of AI was in

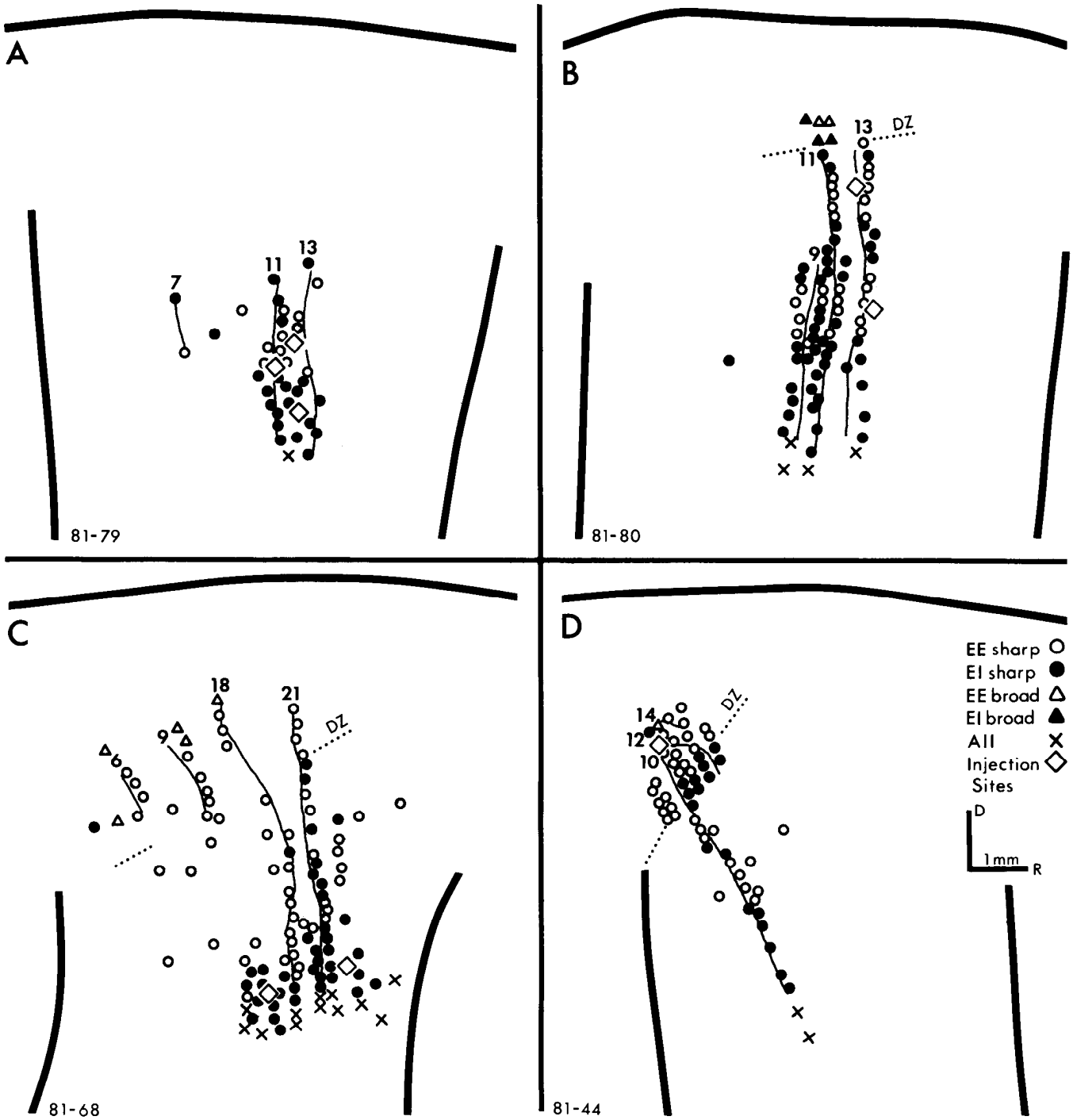

Figure 1. Four examples of functional maps of AI in the right hemisphere; lateral view. *Circles* and *triangles* indicate locations of radial electrode penetrations in which the frequency tuning of recorded neurons was sharp or broad, respectively. *Open* and *solid* symbols indicate, respectively, EE or EI responses to binaural stimulation. *Crosses* indicate penetrations where recorded neuronal activity was characteristic of the second auditory field (AII). *Vertical lines with numbers* indicate isofrequency contours with CFs specified in kilohertz. Locations of injections are indicated with *diamonds*. The location of the ventral border of the dorsal zone (DZ) is indicated in *B*, *C*, and *D*. The map in *A* was not continued dorsally to DZ. *D*, dorsal; *R*, rostral.

the location and size of labeled isofrequency laminae in V. For injections located at cortical sites of representation of successively higher frequencies, labeled isofrequency laminae in V were found farther medial, dorsal, and rostral and grew in total area. A retrogradely labeled isofrequency lamina in V accounts for the representation of a limited range of frequency. Given the tonotopic organization of AI and V, we infer that the thickness of the lamina is roughly proportional to the spread of retrograde tracer along the tonotopic (rostrocaudal) axis of AI.

When injections were restricted to single binaural bands, the resulting retrograde label in the thalamus occupied restricted fractions of the array of neurons that project to an entire cortical isofrequency contour. Nearly all such restricted injections labeled at least a few cells in

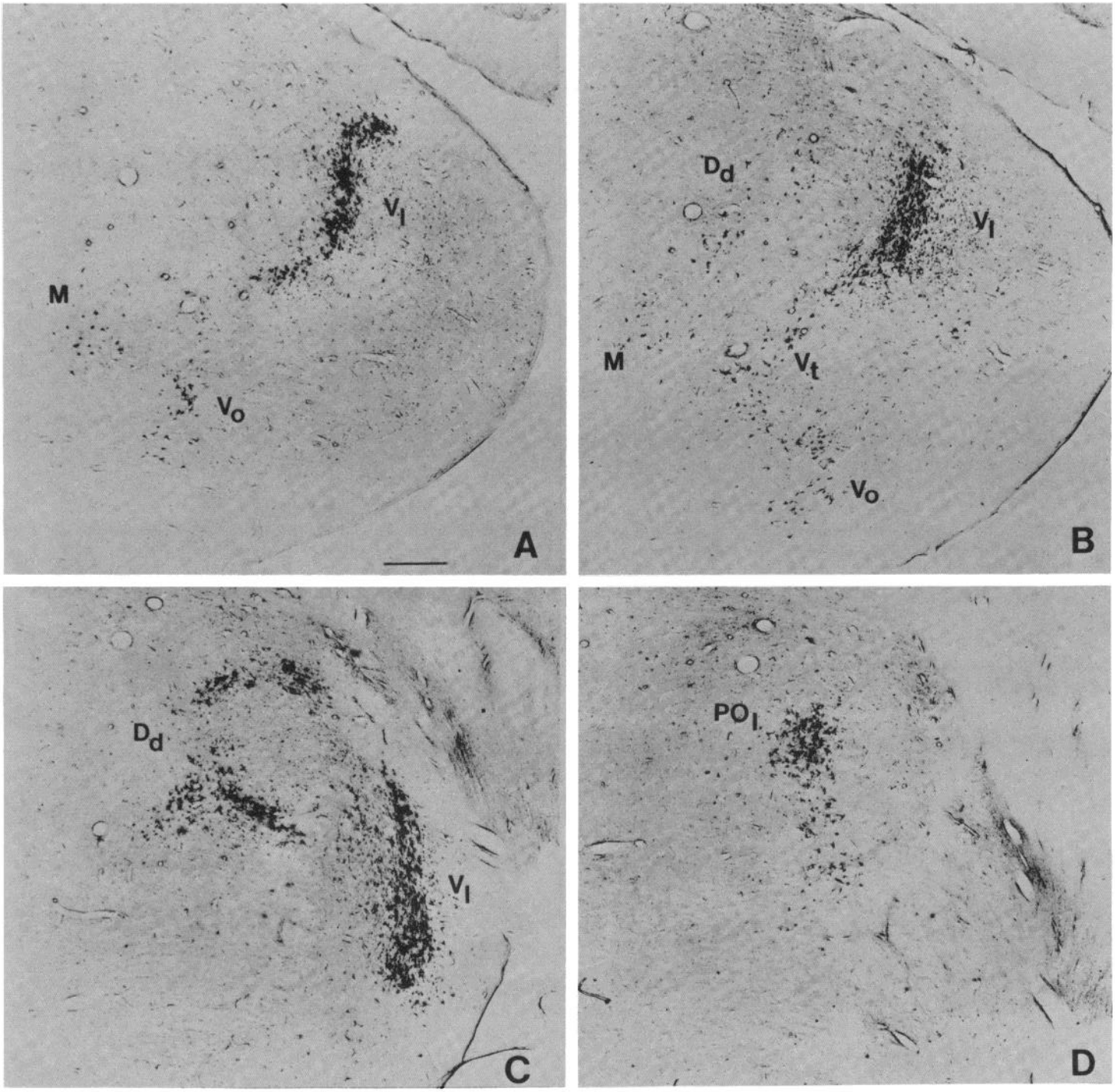

Figure 2. Photomicrographs of the pattern of retrogradely labeled cells in the medial geniculate body resulting from five injections of horseradish peroxidase (HRP) along a 17-kHz isofrequency contour in AI in case 81-70. Fifty-micrometer sections in the Horsley-Clarke coronal plane are shown with no counter-stain. The medial division (*M*), deep dorsal nucleus (D_d), lateral (V_l), ovoidal (V_o), and transitional (V_t) parts of the ventral division (V) and the lateral part of the posterior thalamic group (PO_l) are indicated. Sections are arranged from caudal (*A*) to rostral (*D*). *Scale*, 500 μm.

M, Dd, and POl. The form and amount of label found in those divisions varied considerably between cases. The patterns of label in those divisions were difficult to correlate absolutely with particular AI injection sites, given the apparent variability in these projections and the limited number of injections that were introduced into each binaural band. However, a clear correlation was recorded between injection site locations relative to particular binaural bands and the characteristic patterns of labeled neurons in V. In the descriptions below, we shall focus on band-specific neuronal arrays in V.

The ventral EI band. The AI/AII border was identified in 19 binaural maps. Sectors of the ventral part of AI as large as the representation of about two octaves

were mapped in some experiments. In each of these cases, a band of EI units occupied the ventralmost region of AI. Apart from an occasional anomalous penetration, this ventral EI band appeared to be continuous in its rostrocaudal (tonotopic) dimension in every studied cat. Depending on the aim of a particular experiment, as many as 29 electrode penetrations were placed into this ventral EI band.

The ventral EI band typically was the largest region of EI responses encountered in AI. In a few instances, it narrowed in its dorsoventral (isofrequency) dimension to as little as 0.5 mm, but typically it was 1 to 2 mm wide. In many (but not all) animals, the width of the ventral EI band appeared to increase in more rostral, higher frequency regions of AI.

Injections of retrograde tracers were centered in the ventral EI band in seven cases. In each of these experiments, labeled cells occupied discontinuous areas within an isofrequency lamina in V. In the experiment illustrated in Figure 3, a single injection of HRP was centered in the ventral EI band at the site of representation of 11 kHz. At caudal levels of the projection array, labeled cells formed two discrete clusters in Vl (Fig. 3, *A* and *B*) and a cluster in Vo (Fig. 3*B*). Further rostral (Fig. 3*C*), the ventral label in Vl was continuous through Vt with the labeled cells in Vo. Still more rostral (Fig. 3*D*), the folded sheet of labeled cells in Vl began to straighten to lie in a parasagittal orientation. The labeled array of neurons in the ventral Vl continued nearly to the rostral pole of that division (Fig. 3*E*).

When the discontinuous clusters of labeled cells in V that resulted from ventral EI injections at single frequencies (or restricted bands of frequency) were reconstructed in three dimensions, it was apparent that the pattern of retrogradely labeled cells comprised multiple rostrocaudally oriented columns. Figure 4 shows the pattern of label in V resulting from two injections of NY in the ventral EI band at 18- and 21-kHz loci. The arrays of labeled cells in V resulting from the two injections fused together because of the close spacing of the injections along the tonotopic axis of AI, so that the double injection resulted in a thickening of the projection in V along the thalamic tonotopic dimension. In the illustration, the clusters of labeled cells are outlined and the rostrocaudal axis is expanded by a factor of 5. In the caudal 400 μm of the projection, two columns of label are present in Vl. Further rostral, these columns are joined by a third column in Vo. At some levels, the ventral column in Vl is nearly contiguous to the Vo column. In the rostral 300 μm of the projection, label is restricted to the single column which passes from Vo into the ventral and rostral part of Vl.

This basic pattern was common to all of the ventral EI band injection cases in this series. In V, arrays of neurons projecting to the sites of representation of narrow ranges of frequency always comprised three discrete rostrocaudally oriented columns. At caudal levels, there were two stubby columns in Vl (again, note the 5-fold expansion of the rostrocaudal axis in Fig. 4). The more ventral column was continuous with Vo at some levels and often could be further subdivided along some fraction of its length. Injections into the ventral EI band always produced robust labeling in Vo. The Vo column continued rostrally into the rostral pole of Vl; in some experiments, this column was elongated somewhat in the dorsoventral dimension. In several cases (e.g., Fig. 3), the two columns

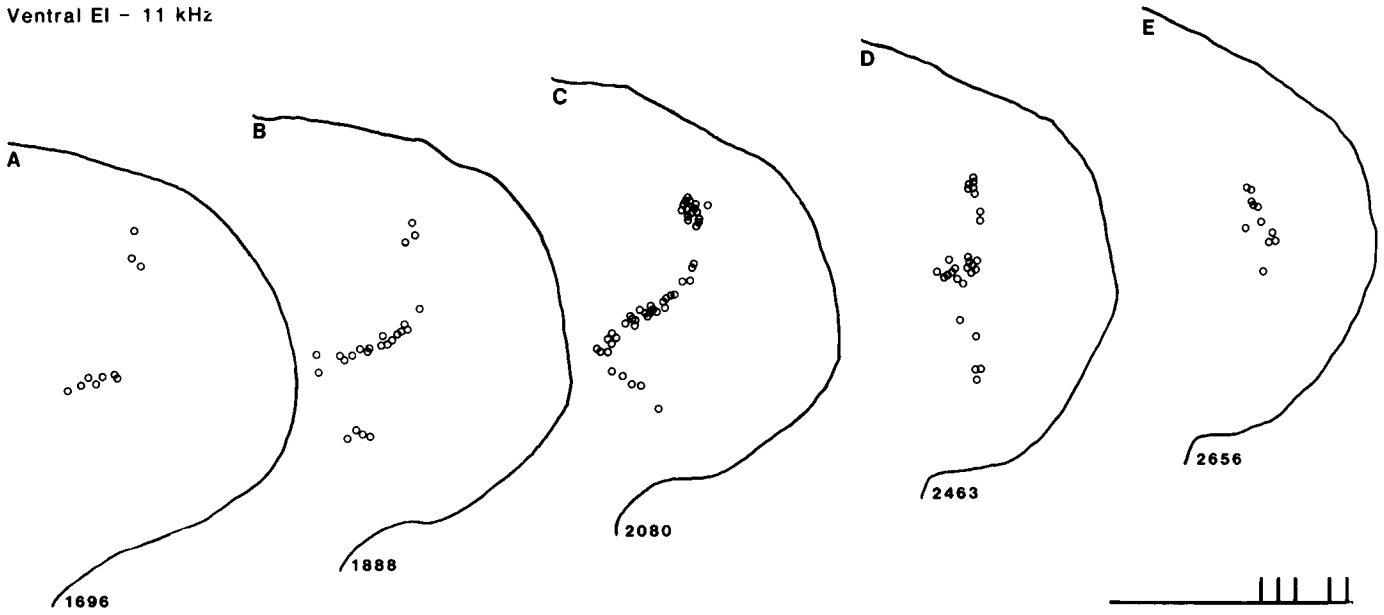

Figure 3. Distribution of labeled cells in V resulting from an injection of HRP in the ventral EI band of AI at 11 kHz; case 81-62 sectioned in the Horsley-Clarke coronal plane. *Open circles* indicate cells retrogradely labeled with HRP. Sections are arranged from caudal to rostral. *Numbers* next to the section outlines indicate distance in micrometers from the caudal aspect of the MGB. *Scale*, 3 mm. *Short vertical lines* on the *scale* represent the rostrocaudal position of each of the illustrated sections, where the *left end* of the *scale* represents the caudal tip of the MGB. *A*, at the caudal pole of the projecting array, labeled cells occupy two columns in Vl. *B*, A cluster of labeled cells is found in Vo. *C*, A line of labeled cells passes nearly continuously from the ventral column in Vl, through Vt, and into Vo. The dorsal column in Vl is still present. *D*, The two columns in Vl are beginning to merge. *E*, Label is restricted to a single lamina in the rostral pole of Vl.

seen in the caudal Vl fused at more rostral levels to form a single column.

The ventral EE band. A ventral band of EE units consistently was identified immediately dorsal to the ventral EI band in AI. Like the ventral EI band, this ventral EE band was continuous along its tonotopic axis and was identified in every case in which the ventral aspect of AI was mapped in detail. This band usually was *not* the widest band of EE responses that was encountered in AI. It ranged from approximately 0.5 mm to 1 mm in its isofrequency dimension. Within a single case, the width of this band could be quite variable, sometimes broadening or narrowing abruptly for short segments of its length.

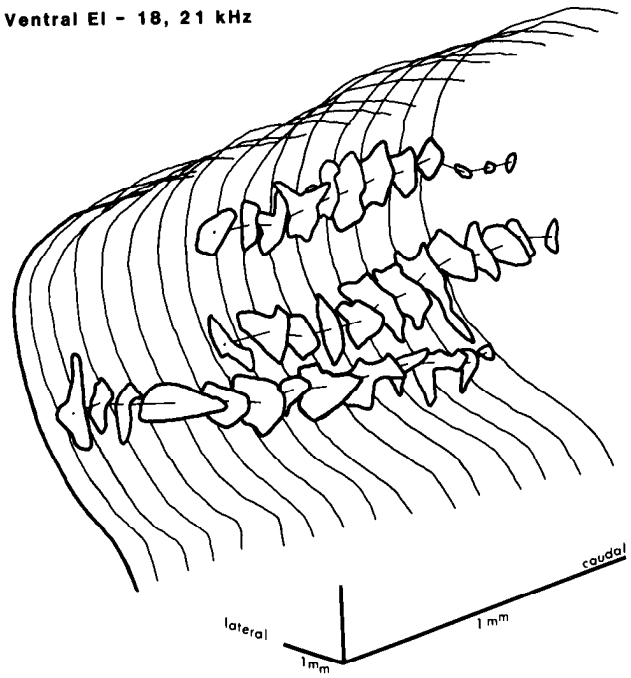

Figure 4. Distribution of labeled cells in V resulting from two injections of Nuclear Yellow (NY) in the ventral EI band at 18 and 21 kHz in case 81-68 (see Fig. 1*C*). The patterns of retrograde label resulting from the two injections are fused because of the close spacing of the injections along the tonotopic axis of AI. Clusters of labeled neurons are indicated with *outlining*. The ventral division is viewed as if from a point inside the thalamus at an angle 45° from the parasagittal plane and 20° above the horizontal plane. The rostrocaudal axis is expanded by a factor of 5. Retrogradely labeled cells occupy two columns in Vl and one column passing from Vo into Vl.

A consistent pattern of retrograde label was observed following five injections of retrograde tracers into the ventral EE band in four hemispheres. In one case (Fig. 5), two injections of retrograde tracers were introduced in the ventral EE band in one hemisphere: NY at 16 kHz and PI at 9 kHz. The labeled cells occupied portions of two parallel isofrequency laminae. At all levels, the projecting array labeled by the injection at the higher frequency lay medial and dorsal to that produced by the lower frequency injection, thus corresponding to the previously described tonotopic organization of Vl (e.g., Colwell, 1977; Colwell and Merzenich, 1975, 1982; Merzenich et al., 1982). In all cases, the arrays of labeled cells in V that resulted from single ventral EE injections could be reconstructed to form single continuous structures. The pattern of NY label resulting from the 16-kHz injection in the case shown in Figure 5 is reconstructed in Figure 6. Again, note that the reconstruction is expanded by a factor of 5 in the rostrocaudal dimension. This projection array shared several features with all of the ventral EE projections. At caudal levels of the projection, a single narrow sheet or column of cells was labeled in the ventral part of Vl. Further rostral, this single column shifted dorsally in Vl and merged with a second, shorter, more ventral cell column. At the rostral pole of the projection, the two merged columns form a continuous parasagittally oriented sheet. Never more than a few (sometimes no) cells were labeled in Vo by ventral EE injections.

The two projecting arrays that were labeled in the case

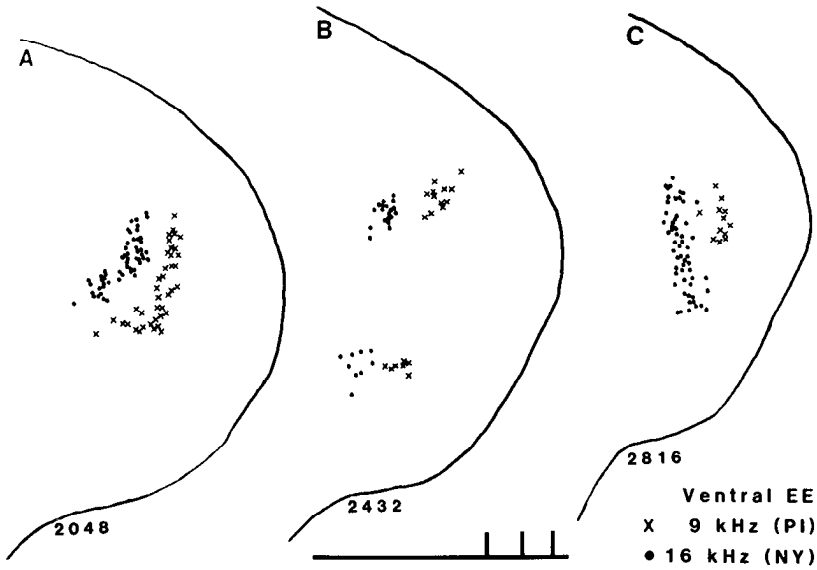

Figure 5. Distribution of labeled cells in V resulting from two injections in the ventral EE band in case 81-81. Propidium iodide (PI) and NY were injected at 9 and 16 kHz, respectively. *Crosses* and *solid circles* indicate cells retrogradely labeled with PI and NY, respectively. For each label, labeled cells are restricted to Vl. *Scale*, 3 mm. Further details are as in Figure 3.

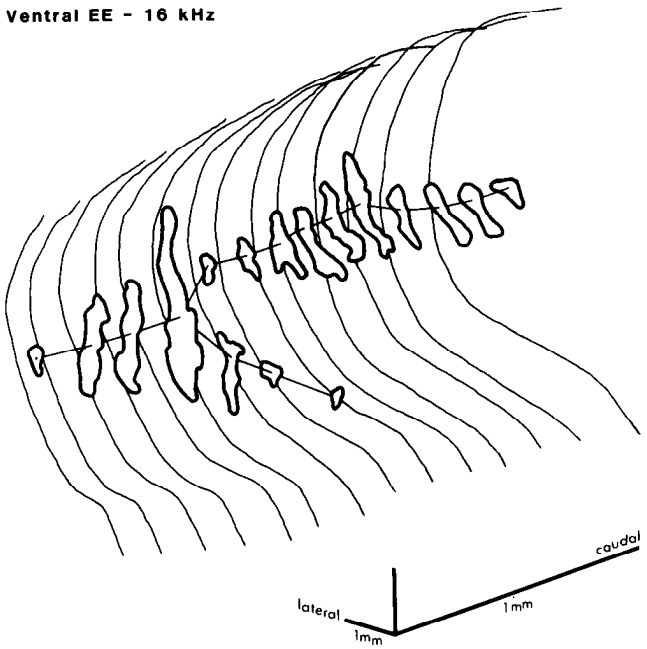

Figure 6. Reconstruction of the distribution of labeled cells in V resulting from an injection of NY in the ventral EE band at 16 kHz for case 81-81 (same as Fig. 5). Further details are as in Figure 4.

illustrated in Figure 5 represent the input from V to two discrete sites along a single ventral EE band. Presumably, the array projecting to the entire rostrocaudal extent of the ventral EE band (i.e., its entire frequency range) occupies a structure that is oriented parallel to the tonotopic axis of V, passing through both of the discrete arrays labeled in the illustrated case.

Segregation in V of the projections to the ventral EI and EE bands. In three cases, the projections to the ventral EE and EI bands were compared within single cats. In each of these experiments, different retrograde tracers were injected into different bands along one isofrequency contour. In the case illustrated in Figure 7, three injections were placed along the 11-kHz isofrequency contour. Nuclear Yellow was injected into the ventral EI band, PI into the ventral EE band, and HRP on the border between the ventral EI and EE bands. All three resulting projecting arrays lay within the same isofrequency lamina in V. The arrays labeled by the two dyes conformed to the patterns described previously as the characteristic ventral EI and EE projections. The most caudal sections (Fig. 7*A*) contained discontinuous clusters of NY-labeled cells from the ventral EI injection (indicated with *solid circles*) but contained no PI label. At more rostral levels (Fig. 7, *B* and *C*), PI-labeled cells from the ventral EE injection (*crosses*) occupied a narrow lamina that was interposed between the columns of NY label. Further rostral (Fig. 7*D*), the fraction of the area of the lamina labeled within PI increased. At the rostral pole of the projection (Fig. 7*E*), the PI-labeled cells filled the dorsal two-thirds of the isofrequency lamina and the NY-labeled cells were restricted to a ventral column.

The HRP injection made in the case illustrated in Figure 7 was introduced on the ventral EI/EE border. The effective spread of the HRP injection was comparable to the spread of either of the dye injection sites alone (judging from the extent of the projections in the tonotopic dimension of V). Yet, the HRP-labeled cells occupied approximately the same area of the isofrequency lamina in V as the NY-labeled cells *plus* the PI-labeled cells. At the most caudal levels (Fig. 7*F*), discrete clusters of HRP-labeled cells were found in correspondence with the ventral EI projection labeled with NY. Rostral to the levels where PI-labeled cells first appeared, the isofrequency lamina is labeled nearly continuously by the HRP injection (Fig. 7, *G* to *J*). The single HRP injection in this case could have reached no more than a fraction of each of the ventral EI and EE bands, *yet it labeled nearly as much of the area of an isofrequency lamina as five injections placed along the entire length of an isofrequency contour* (i.e., see Fig. 2).

The labeled projection in V from the case shown in Figure 7 is reconstructed in Figure 8. This drawing illustrates how the ventral EE projection occupies a single branched but continuous region, while the ventral EI projection forms two discrete regions in Vl plus a third column lying in Vo and the ventral and rostral part of Vl. The patterns of labeled cells in this case are remarkably similar to the patterns of EI- and EE-projecting cells in the cases illustrated in Figures 4 and 6. The reconstruction in Figure 8 also serves to emphasize that, for a given frequency, the ventral EE neuronal projection is centered rostral to the center of the ventral EI neuronal projection array. This observation was confirmed in every case in which injections were placed in the ventral EI and/or ventral EE bands.

The middle bands. In the area of AI above the readily identified ventral pair of binaural bands, the pattern of binaural subdivisions was somewhat more variable. In all cases, EE-responsive units were segregated from EI units and, commonly, binaural response-specific regions appeared to be elongated rostrocaudally. In some experiments (e.g., Fig. 1*B*) there was evidence of two EI bands and one EE band in the area between the ventral bands and the DZ. In other experiments (e.g., Fig. 1*C*), some binaural "bands" clearly were interrupted within this middle region. To aid description, binaural response-specific regions found between DZ and the ventral EE band will be referred to as "middle EE and EI bands" with the *caveat* that these "bands" are much less constant in form than the ventral EE and EI bands.

Injections of retrograde tracers were restricted to single middle bands in several cats in which bands in this middle region could be outlined unequivocally.

In one case, HRP was centered in a middle EI band along the line of representation of 12 kHz (Fig. 9). The band in which this injection was introduced was immediately dorsal to the ventral EE band. The thalamic projection labeled in this experiment was very similar to the pattern that resulted from ventral EI injections in other cats. At caudal levels, two columns of cells were found in Vl (Fig. 9*A*). Further rostral (Fig. 9*B*), the sheet of labeled cells was continuous via Vt to Vo. At the rostral pole of the projection, labeled cells were restricted to a single parasagittally oriented lamina in Vl (Fig. 9*C*).

Injections were restricted within middle EE bands in three successful cases. Projection arrays were somewhat

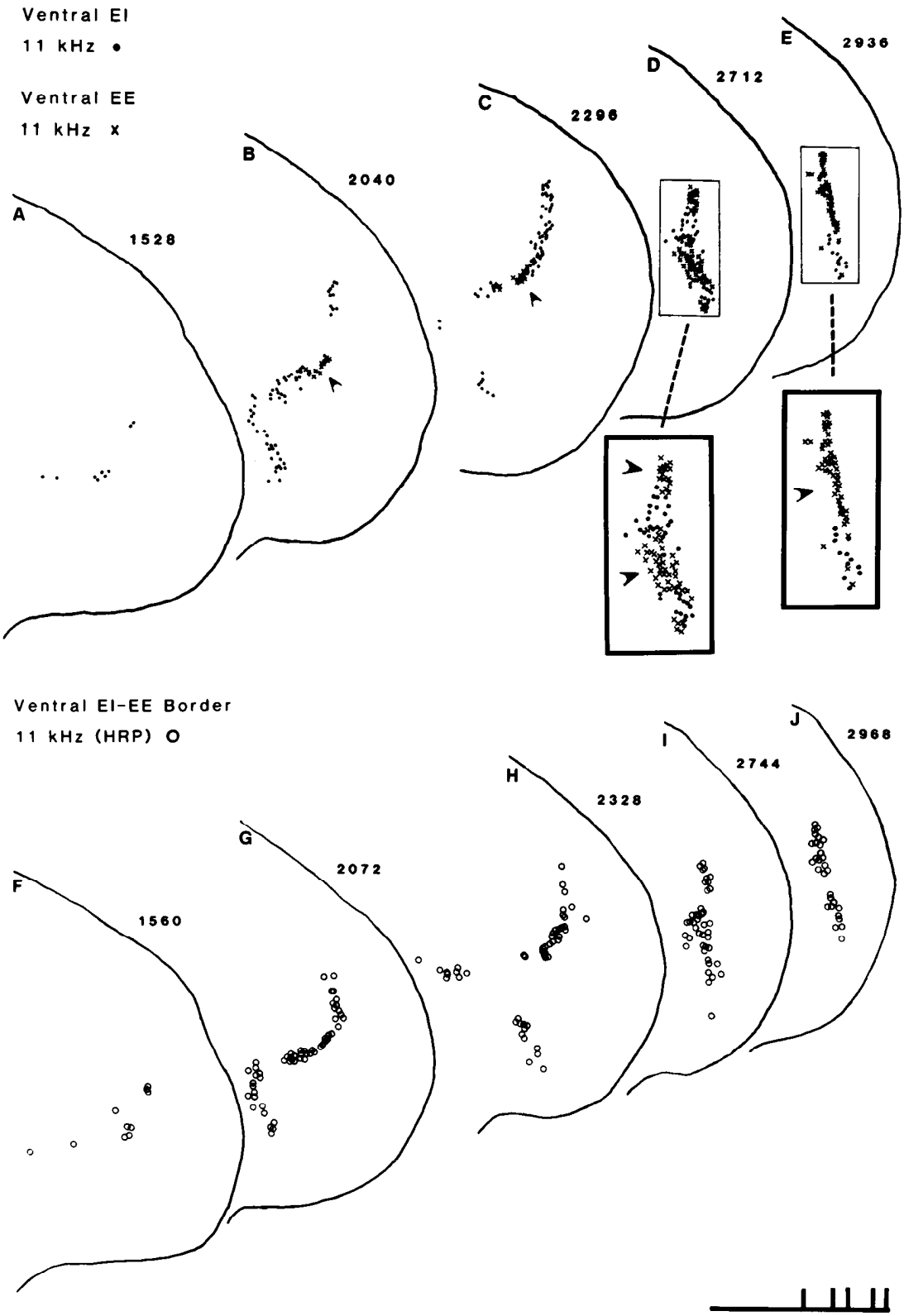

Figure 7. Distribution of labeled cells in V resulting from three injections along an 11-kHz isofrequency contour in case 81-79. NY, PI, and HRP were injected in the ventral EI band, the ventral EE bands, and on the border between the two ventral bands respectively (see Fig. 1*A*). *A* to *E*, *Filled circles* and *crosses* indicate cells retrogradely labeled with NY and PI, respectively. *Arrowheads* indicate clusters of PI-labeled neurons. *Insets* show enlargements of the arrays of labeled cells in *D* and *E*. Note the segregation of clusters of NY- and PI-labeled neurons. *F* to *J*, *Open circles* indicate cells retrogradely labeled with HRP. Note the similarity of the HRP-labeled array to the sum of the arrays labeled with NY and PI. *Scale*, 3 mm. Further details are as in Figure 3.

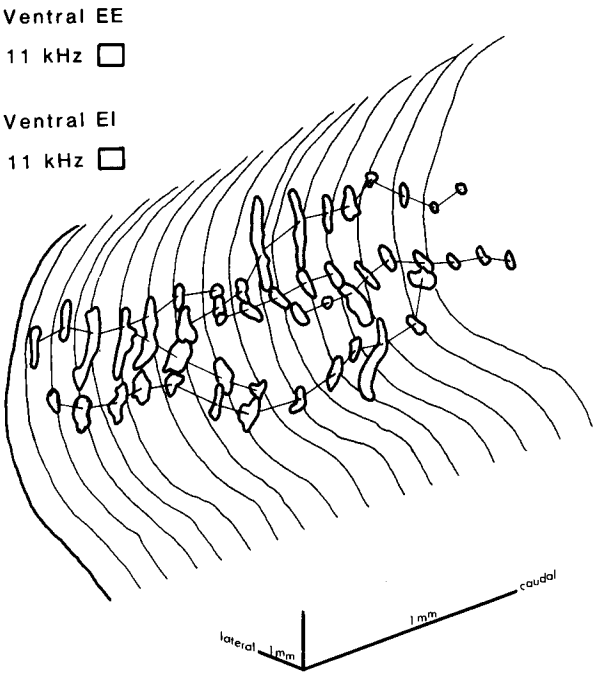

Figure 8. Reconstruction of the distribution of labeled cells resulting from injections of PI and NY into the ventral EE and EI bands, respectively, at 11 kHz. Case 81-79 (same as Fig. 7) is shown. *Open* and *shaded outlines* indicate clusters of PI- and NY-labeled cells, respectively. Note the resemblance of the patterns of NY and PI label to the patterns illustrated in Figures 4 and 6, respectively. Further details are as in Figure 4.

caudal levels (Fig. 10*A*), labeled cells were restricted to a single lamina in the ventral aspect of Vl. This lamina resembled the caudal part of the typical projection to the ventral EE band (e.g., see Fig. 7*B*). A few additional cells were found in the "dorsal cap" of V (Vdc; described further below). The rostral pole of the projection in V occupied a single densely labeled lamina oriented parasagittally (Fig. 10). Only five labeled cells were found in Vo in this cat. In another middle EE injection case (case 81-60; not shown), a very similar pattern was observed. However, in the latter case the number of labeled neurons in Vdc was much greater, and the overall pattern of labeled neurons resembled more closely that resulting from DZ injections (described below). The label in Vl was relatively sparse.

In a third example, an injection of NY was introduced into a middle EE band at 13 kHz (Fig. 11, *solid circles*) and an injection of PI was introduced into the ventral EE band at the same frequency (*crosses*). At caudal levels (Fig. 11*A*), the middle EE projection was restricted to Vdc. Rostrally in V (Fig. 11, *B* and *C*), this cluster elongated ventrally to form a parasagittally oriented lamina. The ventral EE projection pattern in this case was unlike the projections that were demonstrated with five injections in four other cases (described above). Caudally (Fig. 11*A*), the projection occupied a cluster in Vdc. This cluster overlapped extensively with the middle EE projection, although it was centered slightly more ventral. Some doubly labeled cells were observed (indicated with *crosses* superimposed on *solid circles*), al-

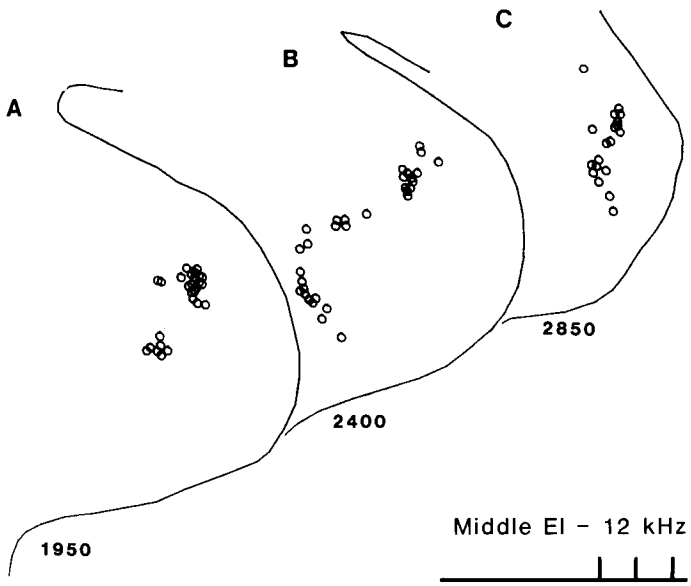

Figure 9. Distribution of labeled cells in V resulting from an injection of HRP in a middle EI band at 12 kHz in case 81-56. *A*, Two columns in Vl. *B*, The ventral column in Vl is nearly continuous through Vt with Vo. *C*, A lamina in Vl. Note the resemblance between this projection pattern and that shown in Figure 3 for a ventral EI injection. *Scale*, 3 mm. Other details are as in Figure 3.

different in detail in each of these cases, but in every experiment, labeled cells apparently were restricted to the regions of V that were labeled by ventral EE and/or DZ injections (described below). Figure 10 illustrates two sections from one of these middle EE injection cases. At

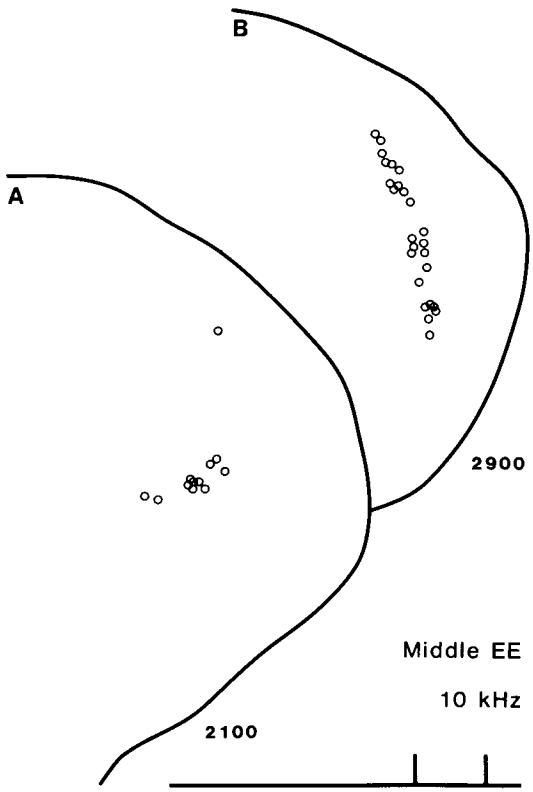

Figure 10. Distribution of labeled cells resulting from an injection of HRP in a middle EE band at 10 kHz in case 81-31, shown in transverse section. *A*, Label is restricted to a cluster of cells in Vl and a single cell in Vdc. *B*, A lamina in Vl. *Scale*, 3 mm. Other details are as in Figure 3.

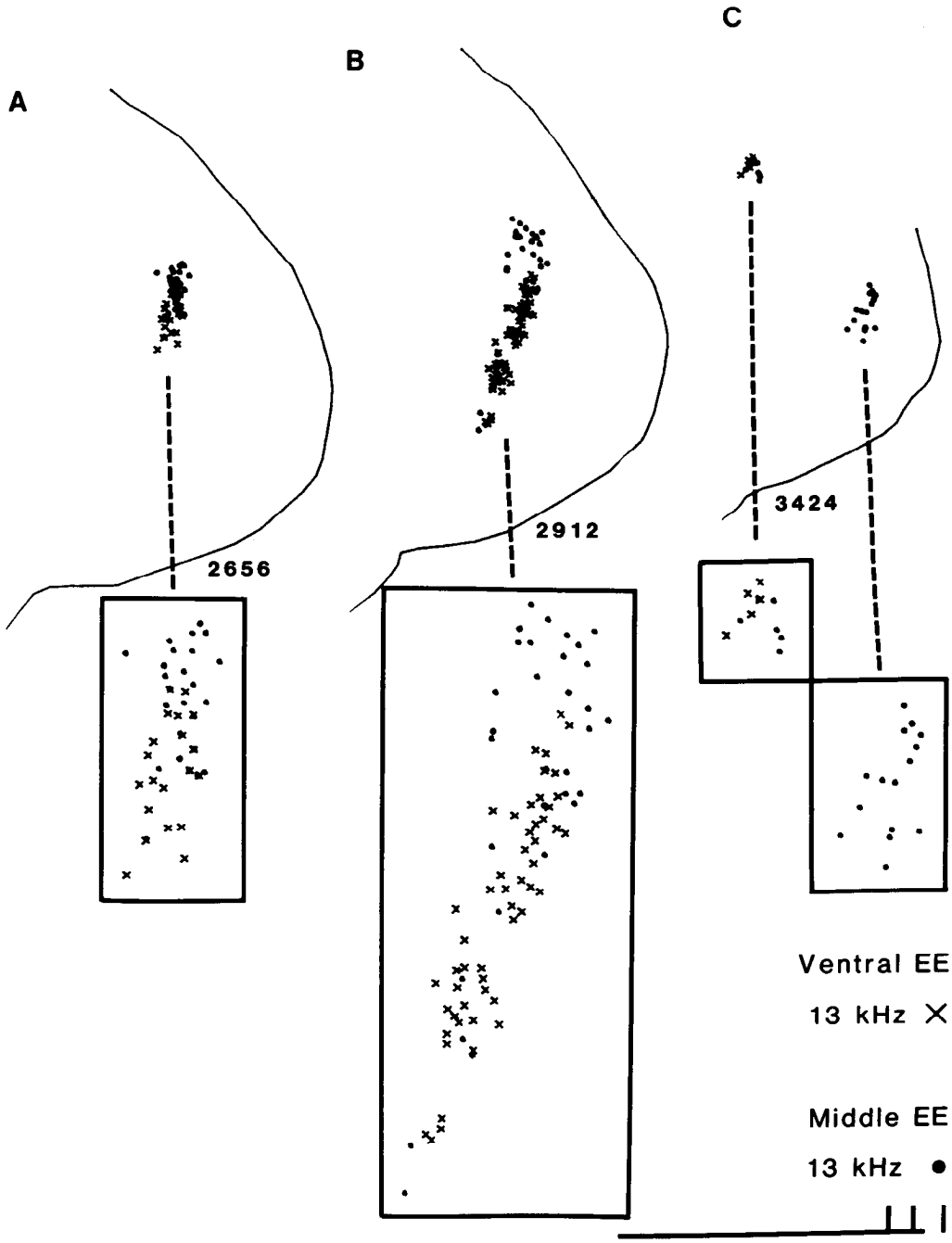

Figure 11. Distribution of labeled cells resulting from two injections along a 13-kHz isofrequency contour in case 81-80 (see Fig. 1*B*). NY and PI were injected into the middle and ventral EE bands, respectively. The ventral EE projection in this case was unlike any of the five other ventral EE projections studied. *A*, Both projections were restricted to Vdc. *B*, Both projections lay within a lamina in the rostral pole of Vl, with the PI (ventral EE) projection centered ventral to the center of the NY (middle EE) projection. *C*, NY-labeled cells were found in Vl and POl, while PI cells are restricted to POl. *Scale*, 3 mm. Further details are as in Figure 3.

though cells singly labeled with PI or NY were much more numerous. Like the middle EE projection, the ventral EE projection occupied a dorsoventrally oriented lamina at rostral levels (Fig. 11*B*), although once again, the center of the ventral EE projection lay further ventral. Each of these injections produced a cluster of labeled cells in POl (Fig. 11*C*). Neither injection resulted in any labeled cells in Vo.

The dorsal zone. In nine cases, microelectrode maps were continued to the dorsal margin of AI across a sector (the dorsal zone; DZ) in which responses differed in frequency specificity and/or in binaural response from those recorded elsewhere in AI. Although there was some variation in the responses that were recorded from this area, it will be treated here as a single cortical region, since: (*1*) responses that were recorded therein frequently differed from those in EE or EI subdivisions as defined previously, (*2*) this area consistently occupied the dorsal margin of AI, and (*3*) there was a consistent pattern of label observed in the thalamus in all cases in which retrograde tracers were injected into this region.

Although unit responses differed from those recorded

elsewhere in AI, no single functional feature was identified as exclusively and universally a characteristic of DZ neurons. In nearly all of the maps which included penetrations in this region, the responses recorded there were unequivocally more broadly tuned for frequency than elsewhere in AI (penetrations where broad tuning was encountered are indicated in Fig. 1 with *triangles*). However, in some cases, broad tuning was encountered only in some penetrations, while responses at nearby penetration sites were sharply tuned (indicated in Fig. 1 with *circles*). In several cases in which tuning was sharp enough for CFs to be determined in DZ, isofrequency contours appeared to turn caudally as they entered DZ, and the representation of high frequencies appeared to be disproportionately large. In other cases, frequency tuning was so broad that CFs could not be measured reliably, but in all penetrations units were encountered that were sensitive to sound stimulation across a broad range of high frequencies. Regardless of the breadth of tuning, there was in all cases at least a general trend of increasing best frequency associated with increasing rostral position.

In most penetrations into DZ, unit clusters could not be driven with monaural stimuli, although vigorous responses were elicited at low threshold for stimuli presented binaurally. Thus, this responsive zone almost certainly was not included in the "AI" defined exclusively with use of monaural stimuli (e.g., see Merzenich et al., 1975). In a much smaller number of penetrations located well within this broadly tuned zone, EI responses were recorded.

The dorsal margin of DZ was explored in only a few cases; thus the exact dimensions of DZ cannot be stated confidently. However, DZ is at least 1 mm wide in the dorsoventral dimension and is bordered dorsally by a region in which no responses could be elicited with the tonal stimuli (and under the state of anesthesia) that were employed in these studies.

Injections of retrograde tracers were introduced into DZ in four cases. Although the response properties of unit clusters in DZ varied somewhat among these cases, the pattern of retrograde label in the thalamus displayed common features. In a representative experiment, illustrated in Figure 12, an injection of HRP was placed at a

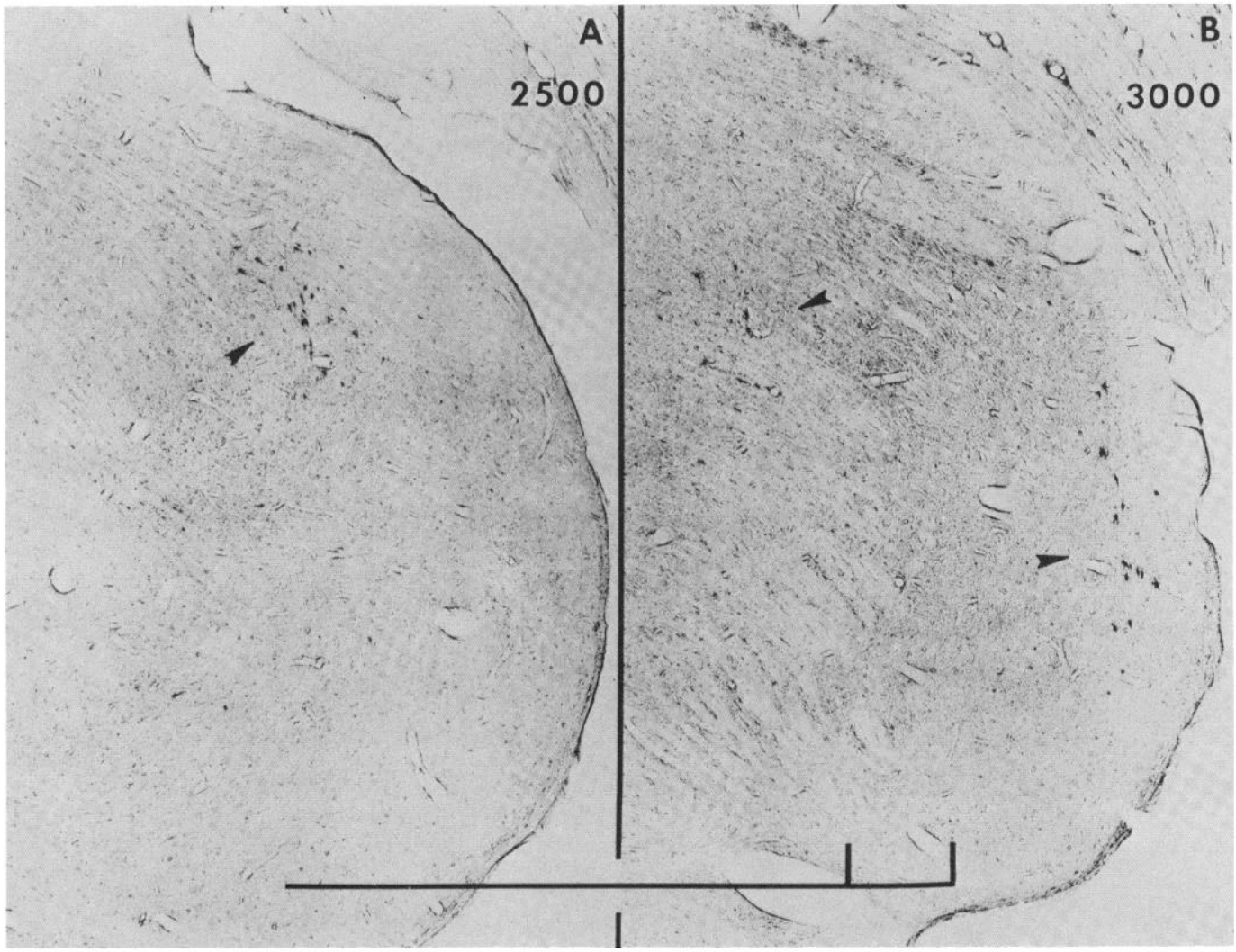

Figure 12. Photomicrograph of the distribution of labeled cells resulting from an injection of HRP into the dorsal zone (DZ) at 10 kHz in case 81-44 (see Fig. 1*D*). *A*, The *arrowhead* indicates a cluster of labeled cells in Vdc. *B*, *Arrowheads* indicate a lateral lamina of cells in Vl and a more medial cluster of cells in POl. *Scale*, 3 mm.

site in DZ where unit clusters were tuned somewhat more broadly than is typical of AI but had best frequencies around 10 kHz. As was true of all DZ injection cases, the region of dense labeling in the projection in V was restricted in its rostrocaudal extent to the rostral half of the domain of ventral EI neuronal projections at comparable frequencies. The caudal pole of the projection consisted of a dense cluster in the "dorsal cap" of V (Vdc; Fig. 12*A*; Morest, 1965). This cluster of cells lay immediately lateral to the auditory radiation in the dorsal aspect of V. The caudal aspect of the projection appeared in the same coronal plane as the rostral pole of Vo. At more rostral levels in all DZ injection cases (Fig. 12*B*), labeled cells in V were found further ventral and lateral, occupying a lamina oriented parasagittally. This lamina was similar in form and location to that labeled by ventral EE injections, although in some cases it appeared that labeled cells in the rostral Vl were distributed somewhat more diffusely in the mediolateral (tonotopic) dimension than was observed following comparably sized injections in the ventral EE band. All DZ injections produced a cluster of labeled cells in M and a single column of labeled cells in Dd that could be followed rostrally into POl (Fig. 12*B*).

In addition to the dense cluster of labeled cells in Vdc, many sections in DZ injection cases contained a few cells scattered throughout the caudal levels of Vl and Vt. These cells might be sources of input to the few sites in DZ at which EI responses were recorded. No more than a few cells were found in Vo in any DZ injection case. The pattern of label in V found in the case illustrated in Figure 12 is reconstructed in Figure 13. The areas of dense labeling are indicated with *outlining*. The limited rostrocaudal extent of this projection pattern was typical of DZ projections.

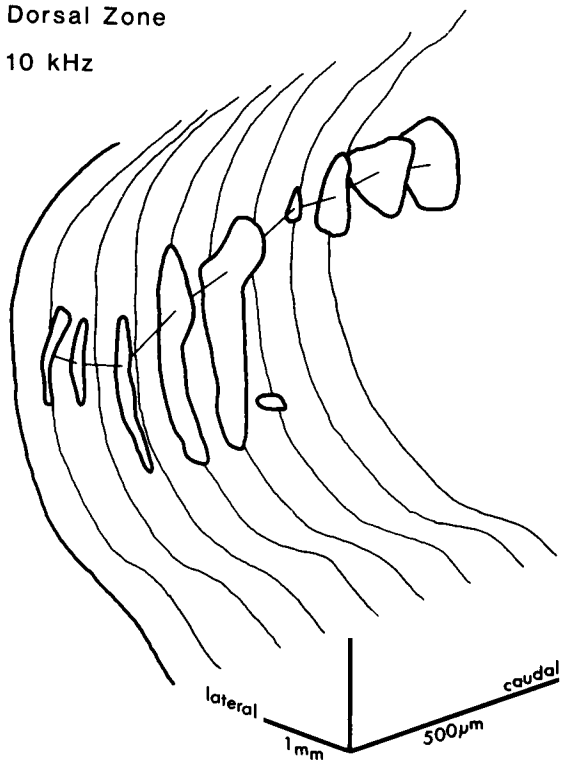

Figure 13. Reconstruction of the distribution of labeled cells resulting from an injection of HRP in DZ at 10 kHz in case 81-44 (same as Fig. 12). Note the limited rostrocaudal extent of this projection. Further details are as in Figure 4.

Summary of differences in the thalamic distribution of neurons that project to different binaural response-specific regions. The graph shown in Figure 14, *A*, *C*, *E*, *G*, and *I* illustrate for five representative cases the distribution of cells among subdivisions of V as a function of rostrocaudal position. The *abscissa* represents the locations of labeled neurons relative to the caudal tip of the MGB. The *ordinant* represents the number of cells found in each section, expressed as a percentage of the total number of cells found in V for each case. The *open arrowhead* along the *abscissa* of each graph indicates the position of the section which contains the median cell number in that case. These graphs illustrate that the caudal pole of the projection from V to AI is occupied by cells that project to EI bands, while the rostral pole is occupied more predominantly by neurons which project to EE bands. The neuronal arrays that project to EE bands and to DZ are centered rostral to those that project to EI bands.

The absolute numbers of labeled cells found in V, M, and Dd/POl in these cases are plotted in Figure 14, *B*, *D*, *F*, *H*, and *J*. These graphs demonstrate that: (*1*) the principal projection (in terms of cell numbers) to *any* site in AI is from V, (*2*) the projection from M, although identified in most cases by a few scattered cells, never constitutes more than a minor fraction of the total population of projecting neurons; and (*3*) neurons that project from Dd/POl can account for nearly half of the input to a site in AI in some cases. The numbers of Dd/POl neurons projecting to AI sites varied considerably between the cases. No consistent relationship between the binaural band that was injected and the resulting pattern of label in Dd/POl has yet been identified.

Discussion

Previous studies of the thalamic projections to the auditory cortex (AI) of the cat have demonstrated a systematic, *tonotopic* organization in the projection from the ventral division (V) of the medial geniculate body (MGB). The AI sites of representation of successively higher frequencies derive input from successively more medial folded sheets of neurons which cross all of the subdivisions of V (Colwell, 1977; Colwell and Merzenich, 1975, 1982; Winer et al, 1977; Andersen, 1979; Andersen et al., 1980a; Merzenich, 1982). In the current study, retrograde tracers introduced in relation to physiologically identified boundaries of binaural bands in AI were used to define the organization of the projection from V to AI in the orthogonal, *isofrequency* dimension of the representation. These experiments reveal a complex yet orderly relationship between thalamic subdivisions defined by their cortical projections and the functionally defined binaural bands of AI.

Specifically, the results indicate the following. (*1*) The ventral division of the MGB also is functionally subdivisible, at least in the sense that the sources of input to the functionally defined subdivisions of AI occupy regional subdivisions in V. (*2*) Restricted segments of EI bands in AI derive their principal inputs from three discrete columns of neurons. Two such columns pass across the lateral part (Vl) of V; one crosses from Vl into the ovoidal

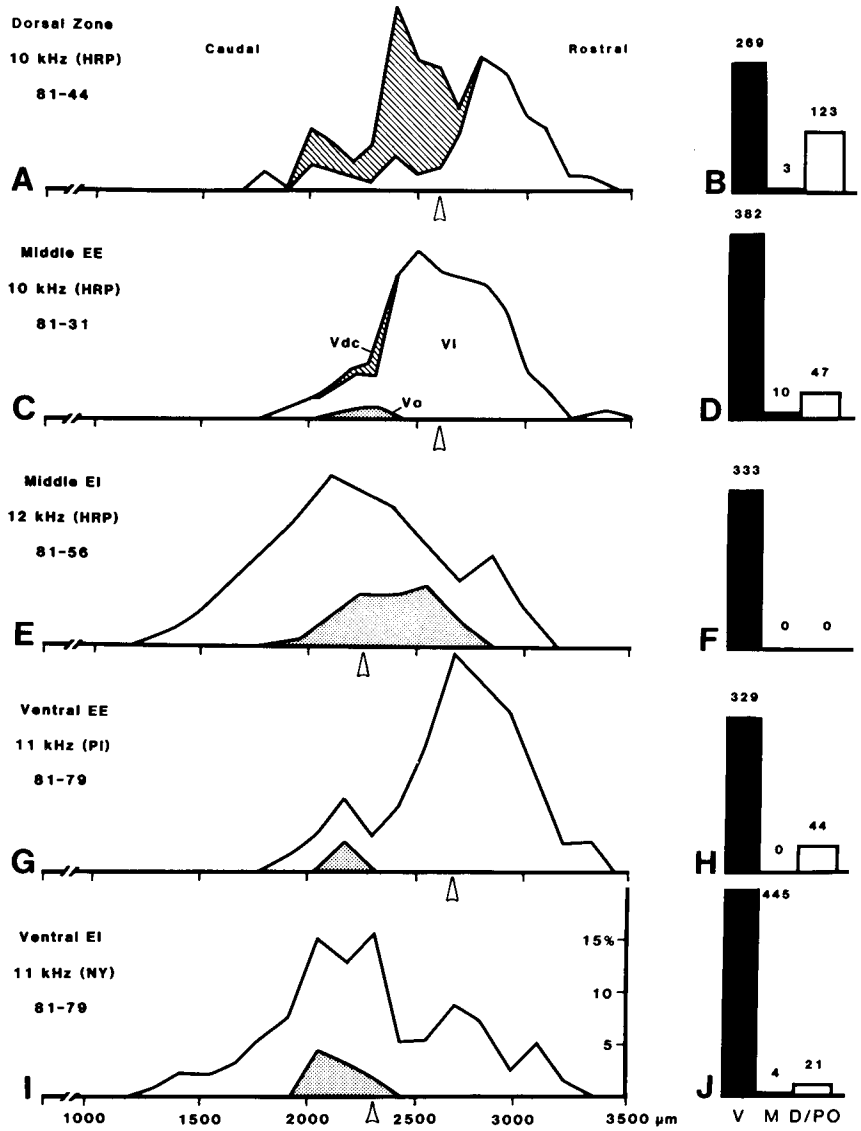

Figure 14. Summary of the distribution in the thalamus of cells projecting to identified binaural bands. Examples of the projections to DZ and middle and ventral EE and EI bands are given. *A*, *C*, *E*, *G*, and *I*, Normalized number of cells in Vo, Vl, and Vdc (*shaded*, *unshaded*, and *hatched areas*) as a function of position in micrometers rostral to the caudal tip of the MGB. *Arrowheads* indicate the sections containing the median cell number for each case. *B*, *D*, *F*, *H*, and *J*, Absolute numbers of labeled cells found in major divisions of the auditory thalamus. Counts for Dd and POl have been combined. Counts for cases 81-44, 81-31, and 81-56 are based on alternate 50-μm sections. The count for case 81-79 is based on every fourth 32-μm section.

part (Vo) of V. (*3*) Restricted sites along EE bands in AI derive their input from a continuous, branched sheet of neurons in the dorsal cap (Vdc) and Vl. (*4*) Binaural bands in AI of the same functional class appear to derive their input from the same restricted sectors of V. (*5*) The ovoidal part of V projects heavily to EI bands but provides little input to EE bands, suggesting that it might be predominantly an EI subdivision. (*6*) Arrays of neurons that project to loci in EE bands are centered further rostral within V than are those that project to loci in EI bands. (*7*) The pattern of retrogradely labeled cells that resulted from an injection centered on an EE/EI border was indistinguishable from the sum of the patterns resulting from two similarly sized injections that were centered within an EE and an EI band. Thus, common EE and EI projections must diverge to fill the dorsoventral extent of individual respective EE and EI bands. (*8*) A dorsal zone (DZ) of AI with special response characteristics was identified in a number of cases. Neuronal responses there were marked by relatively broad frequency tuning and, commonly, by insensitivity to monaural stimulation (yet driven strongly by binaural stimulation). The thalamic sources to DZ overlapped with those of EE regions which displayed more conventional response properties.

The basic organization of the isofrequency dimension of AI and V within the representation of high frequencies is illustrated schematically in Figure 15. An idealized lateral view of AI is shown (Fig. 15*A*). The 10-kHz isofrequency *lamina* in the ventral division of the MGB which projects to the 10-kHz *contour* in AI is shown unfolded into the plane of the page (Fig. 15*B*). The EI, EE, and DZ subdivisions in AI and the corresponding sources of input in V are indicated, respectively, with

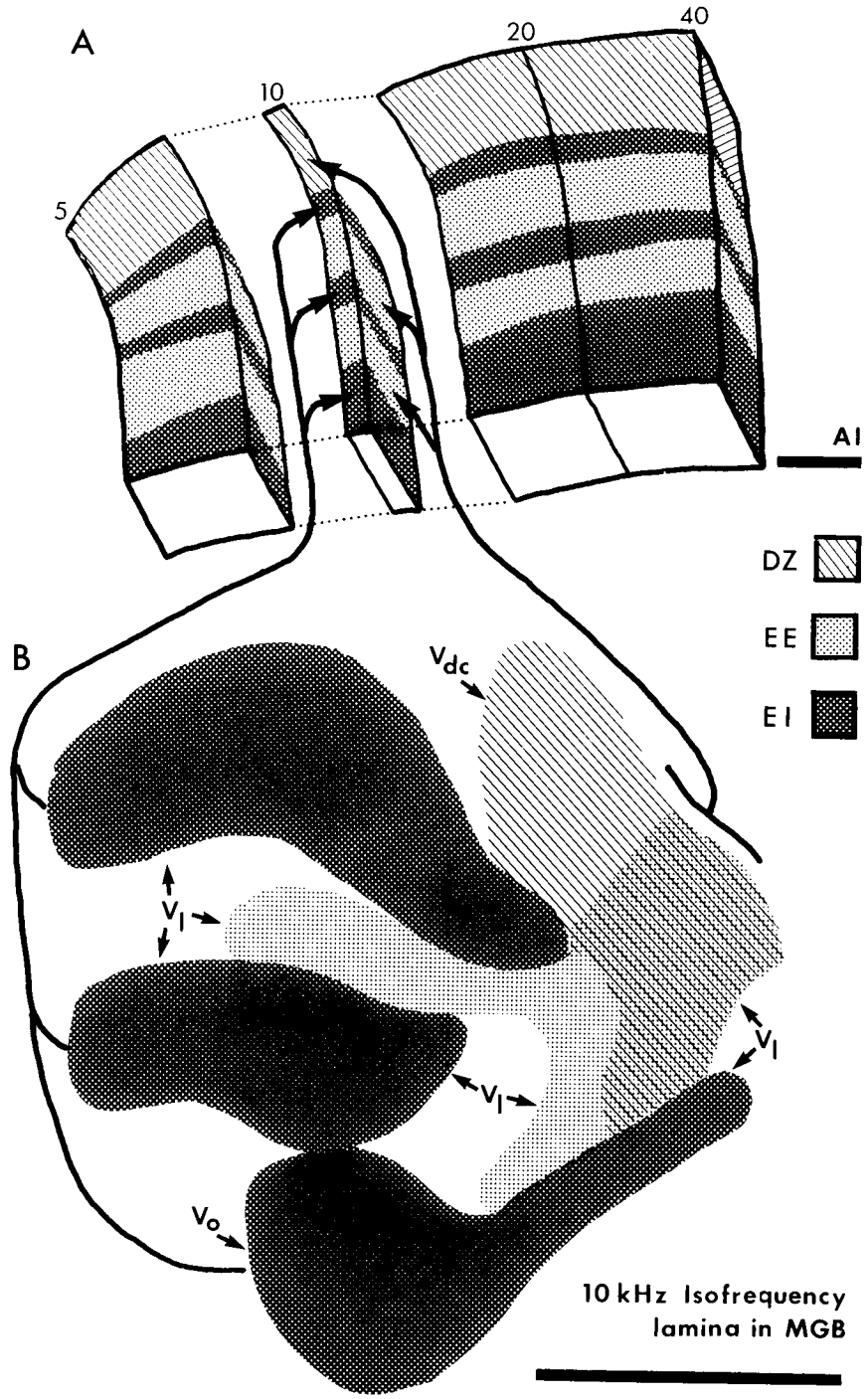

Figure 15. Schematic drawing of the topography of the projections from the ventral division (V) to AI. *A*, Idealized binaural and tonotopic map of the sector of AI which represents 5 to 40 kHz in the right hemisphere. A 10-kHz isofrequency contour is shown in isolation. The illustrated rostrocaudal thickness of the contour is arbitrary; presumably, the representation of any single frequency is infinitesimally thin. *B*, A 10-kHz isofrequency lamina in V flattened onto the plane of the page. *Dark shading* indicates EI bands in AI and their sources of input in V. *Light shading* indicates EE bands and sources. *Diagonal lines* indicate DZ and its sources. *Scale* for each part, 1 mm. The approximate locations of Vo, Vl, Vt, and Vdc are indicated. Note that the regions of cells that project to EE bands and to DZ overlap in the rostral pole of Vl.

dark shading, *light shading*, and *cross hatching*. Of course, the intrinsic organization of V that is represented in figure 15*B* extends in the tonotopic dimension (i.e., out of the plane of the page). The binaural class-specific projection sources in V constitute large slabs of projecting neurons, each sending projections to the representation in AI of at least the three highest octaves of the audible range. The extension of these large functional subunits to frequencies below 3 to 5 kHz is questionable, as is discussed below.

Relation to earlier anatomical studies. The results of these tracing studies are largely consistent with recent descriptions of the basic patterns of projections of the MGB to AI. In addition, by distinguishing the arrays of

neurons that project to binaural bands, these results show some of the complex, hitherto unrevealed organization that is contained within the isofrequency dimension of the V to AI projection. This more detailed information also provides a basis of understanding of some of the apparent discrepancies in the existing literature in descriptions of the thalamic sources to AI.

Studies that relied on anterograde or retrograde degeneration techniques for neuroanatomical tracing identified the "principal division" (the ventral division and deep part of the dorsal division of Morest, 1964) of the MGB as the major thalamic source of input to AI. A more diffuse input originating from within the magnocellular division (which included Morest's medial division, M) also was identified (e.g., Rose and Woolsey, 1949; Neff et al., 1956; Wilson and Cragg, 1969; Niimi and Naito, 1974). No projection from the posterior thalamic group to AI was demonstrated with degeneration techniques, even though studies revealed ascending inputs from the inferior colliculus to the lateral part of the posterior group (POl; Moore and Goldberg, 1963) and descending inputs to POl from the auditory cortex (Jones and Powell, 1971).

The thalamic projection to AI has been defined in several earlier studies in which HRP was used as the retrograde tracer. The basic AI projection first was studied with this method by Colwell and Merzenich, who introduced injections of HRP at known best frequency sites located well within the physiologically defined borders of AI (Colwell, 1977; Colwell and Merzenich, 1975, 1982). They found that an intermediate-sized HRP injection placed in AI resulted in a continuously labeled sheet of neurons in V, with an additional column of cells labeled in the deep part of the dorsal division (Dd) and POl and a pocket of cells labeled in M. They also demonstrated the basic topography of interconnection across the tonotopic axes of AI, V, and Dd. Winer et al. (1977) and Andersen and colleagues (Andersen, 1979; Andersen et al., 1980a) described similar projecting arrays, the latter group also using functional mapping techniques to characterize injection loci in regard to tonotopic organization. Winer et al. (1977) illustrated the result of one relatively dorsal injection that was quite different from cases illustrated in other studies. In that cat, the labeled MGB cells were located rostrally in V, with a dense cluster of labeled neurons in (what we take to be) Vdc and a rostral parasagittal sheet of neurons. Indeed, the present experiments indicate that this array almost certainly resulted from an injection that was restricted to DZ.

Niimi and Matsuoka (1979) also used HRP as a retrograde tracer in an attempt to demonstrate the thalamic projections to AI. Their results were consistent with the fundamental tonotopic organization observed in the current study. However, they found that dorsal injections in AI tended to result in projections located dorsally in V, while more ventral AI injections tended to result in more ventral projections. They concluded that the dorsoventral dimension of V might be represented in the cortex as a continuous gradient in the dorsoventral dimension of AI. In our results, the projections resulting from some dorsal injections were located further dorsal in V than the projections resulting from other more ventral injections (e.g., the DZ projections compared to the ventral EE projections). However, the results of other injections (e.g., the ventral or middle EI injections) are incompatible with the existence of any simple continuum in the thalamocortical topography of that dimension.

In a study by Colwell and Merzenich (1975, 1982; Colwell, 1977), microelectrode mapping was used to position injections of HRP in known relation to the tonotopic organization of AI, as in the current study. Single, moderately sized injections of tracers introduced into AI produced single, continuously labeled isofrequency laminae in V. Injections placed at two loci along the *tonotopic* axis in AI produced two such laminae in V. Two or more injections centered at different points along the *isofrequency axis* in AI resulted in no significant change in the labeled isofrequency contour. These results suggested that projections from all across isofrequency laminae in V *converge* onto restricted segments of isofrequency contours in AI and, conversely, that restricted loci in V send projections that *diverge* to sites distributed all along isofrequency contours. Single small injections placed at high frequency loci sometimes resulted in a discontinuous, banded pattern of label in V. Colwell and Merzenich (1975, 1982; also see Merzenich et al., 1982) interpreted that result to indicate that there was some sort of repeating subunit within the AI projection from V that was smaller than the effective spread of their moderately sized injections. Andersen et al. (1980a) also found that single small injections of HRP sometimes labeled multiple, discrete, rostrocaudally oriented columns of cells in V. Merzenich et al. (1982) suggested that the discontinuous columns labeled by small injections placed in the high frequency area of AI might be regions of V that project to single binaural interaction bands in AI. That hypothesis has been confirmed in the current experiments in which injections were introduced in known relation to single binaural bands.

Relationship to physiological studies of the auditory thalamus. Neurons in the MGB exhibit binaural responses that are similar to those recorded in AI (Aitkin and Webster, 1972; deRibaupierre et al., 1975; Calford and Webster, 1981). However, physiological studies of the MGB have failed to demonstrate any segregation of EE- and EI-responding neurons that is comparable to the functional subdivision of V that is suggested by the current results. Aitkin and Webster (1972) reported no systematic distribution of binaural responses within Vl. The proportion of EE to EI neurons encountered in Vl and Vo was approximately equal, contrary to the prediction from the current anatomical results that most of the units in Vo should display EI or monaural responses. However, the large proportion of EE responses recorded in Vo might have resulted from the apparent oversampling of units in Vo tuned to low frequencies (most of the reported EI units in the MGB have high CFs; Aitkin and Webster, 1972). The discrepancy also may lie with the definition of Vo itself. Physiologically controlled projection studies of Colwell and Merzenich (1975, 1982) strongly indicated that Vo was predominantly a high frequency nucleus, consistent with the present results and contrary to the physiological results of Aitkin and Webster (1972).

deRibaupierre et al. (1975) concluded that binaural response properties apparently were distributed randomly in Vl. In contrast, Calford and Webster (1981)

reported that units with different binaural properties were segregated in many microelectrode tracks across the MGB (they restricted attention to the caudal part of the dorsal division and to V), but they saw no indication of rostrocaudally oriented binaural columns. In the case in which binaural responses are illustrated along reconstructed electrode tracks, no clear conclusions about segregation of classes of binaural units can be drawn.

The failure of physiological studies to demonstrate a layered separation of EE and EI units in the MGB could be interpreted in the light of the present results in several ways. First, the complex folded structure of isofrequency laminae in V, particularly in the caudal aspect (through which, it appears, most electrode tracks have passed), would confound any attempt to demonstrate the binaural organization within such a lamina. Second, the segregation of thalamic cells which project to different functionally defined cortical subdivisions may not reflect an analogous segregation of functionally distinguishable thalamic cells. Thus, for example, a population of EE-responding neurons in Vo might project only to cortical sites outside of AI, or there might be EE-responding units in Vo that provide an inhibitory or otherwise masked projection to cortical EI bands.

The existence of functional subdivisions in the MGB is strongly supported by an observation by Andersen et al. (1980b). They found that injections of anterograde tracer restrieted to response-specific regions of the central nucleus of the inferior colliculus resulted in discontinuous labeling in the MGB. Taken with these cortical projection studies, it would appear likely, then, that the physiological mapping studies in the MGB simply have not been refined enough to demonstrate the complex three-dimensional distribution of binaural neurons in V.

Toros et al. (1979) described a systematic variation in the number of cells receiving excitatory ipsilateral input associated with position along the rostrocaudal axis of Vl. Those authors classified units as "contralateral dominant" or "ipsilateral dominant" and found that the percentage of the sampled population displaying ipsilateral dominance rose to a maximum in the anterior pole of the middle third of Vl. This observation might correspond to our finding that the center of the array of cells that project to EE bands is located rostral to the center of the EI projection (e.g., see Fig. 15).

It should be noted that the low frequency segment of AI (especially the area representing frequencies below about 2.5 kHz) is largely, probably entirely, EE in response character. Correspondingly, Colwell and Merzenich (1975, 1982) and Andersen et al. (1980a) observed discontinuous thalamic arrays resulting from high frequency but *not* from low frequency AI injections. The current description of a layered ventral division almost certainly applies only to the higher frequency (more medial) aspect of V.

In many penetrations in DZ, the units that were encountered were broadly tuned for frequency. Might this broad tuning in DZ be accounted for by an input from a population of broadly tuned EE units in the thalamus? The major sources of thalamic input to DZ are Vdc and the rostral pole of Vl. No discrete population of broadly tuned neurons has been described in V. However, judging from the illustrated electrode tracks (Aitkin and Webster, 1972; Calford and Webster, 1981), there have been few or no recordings made from Vdc. Cells in Vdc and rostral Vl also constitute a major part of the projection to the ventral and middle EE bands in which units are sharply tuned. For this reason it is unlikely that a large percentage of the cells in Vdc or the rostral pole of Vl are broadly tuned. It appears more probable that the broad tuning in DZ results from a convergence of input from a population of sharply tuned neurons whose CFs vary within the population. This hypothesis is consistent with the observation that the sheet of labeled cells in the rostral pole of Vl resulting from DZ injections tended to be thicker and more diffusely labeled than that resulting from comparably sized injections in other EE subdivisions.

Topography of projections along isofrequency contours within AI subdivisions. Historically, Tunturi (1950, 1952) hypothesized that there might be a single systematic binaural representation within AI, constituting the probable basis of a map of sound location. A map of target range and other systematic auditory cortical maps recently have been described within the auditory cortex of the mustache bat (e.g., Suga and O'Neill, 1980, O'Neill and Suga, 1982). The current studies demonstrate that there is no single, continuous binaural representation in the higher frequency sector of AI of the cat, nor is there a systematic "map" explicit in the projection from V to the isofrequency dimension of AI. The data also bring into question whether there is an orderly topographic pattern of projection within the isofrequency dimension of the *subunits* of AI. For example, an injection deliberately centered on the border between the ventral EE and EI bands resulted in a retrogradely labeled array in V that was indistinguishable from the sum of the two arrays that resulted from injections centered within each band. Such observations are limited, but they strongly indicate that there is no point-to-point spatial ordering of projections from sites within EE or EI thalamic projecting zones to sites along the isofrequency dimension of EE or EI cortical subdivisions.

All cortical EI injections resulted in labeling in arrays in V which comprised the same three subunits: two columns in Vl and a column passing from Vo to the rostral Vl. Although we cannot rule out the possibility of variation in the extent of labeling within each thalamic subunit, the same set of subunits always was labeled regardless of the particular EI band that was injected. In contrast, there was more variation in the EE- and DZ-projecting arrays. All EE and DZ sites along a given isofrequency contour derive their input from regions of the same continuous sheet in Vl and Vdc, yet the relative amount of label that was found in each area of the sheet depended on the particular band containing the injection site. All EE and DZ injections resulted in labeling in the same part of the rostral pole of Vl. However, Vdc was labeled by all DZ injections and to a varying extent by middle EE injections, but almost never by ventral EE injections. Conversely, the lamina of cells in Vl which formed the most caudal part of the EE-projecting sheet was labeled after all but one of the ventral EE injections, some of the middle EE injections, and none of the DZ injections. This somewhat systematic variation in labeling is consistent with the observation of qualitative differences in response properties within the EE class

(Kitzes et al., 1980; Phillips and Irvine, 1981) and with the suggestion from physiological studies that different subclasses of EE neurons are segregated within different EE bands in AI (Imig and Adrian, 1977; Merzenich et al., 1979; the current results).

The relationship of the dorsal zone to AI. The dorsal zone appears to be a part of AI, since: (*1*) it appears to fall within the cytoarchitectonic boundaries of AI (Rose, 1949; Rose and Woolsey, 1949; Sousa-Pinto, 1973) and (*2*) its thalamic sources of input coincide with those of other predominantly EE regions in AI within which neurons are sharply tuned. It probably was not included in "AI" as defined by Merzenich et al. (1975) who used contralateral monaural stimulation. The dorsal zone apparently was excluded from AI in the mapping experiments of Reale and Imig (1980) because of the broad tuning of neurons and because of its apparent discrepancy with the tonotopic organization in "AI;" it was termed by them the "dorsoposterior region of the peripheral auditory belt." A major division of the peripheral auditory belt, the second auditory field (AII), shares with DZ the property of broad frequency tuning, yet AII receives its major thalamic input from a discrete part of the MGB (Andersen et al., 1980a) that is not labeled by injections of retrograde tracers anywhere in AI, including DZ. If our interpretation is correct, the basic frequency organization described for "AI" by Merzenich et al. (1975) and by Reale and Imig (1980) applies to all but DZ. That is, there is a significant area within AI (as defined in the current study) in which tuning is broad and characteristic frequencies are difficult to measure reliably. Perhaps this discrepancy in frequency specificity between DZ and the balance of AI has contributed to historical descriptions of "AI" as lacking precise tonotopic organization (Evans et al., 1965; Oonishi and Katsuki, 1965; Goldstein et al., 1970). Indeed, most of AI *is* strictly tonotopically organized, but within this significant dorsal sector, such order would be difficult to demonstrate.

How does the functional subdivision of AI reflect the organization of the ascending auditory neuraxis? The current observations support the hypothesis that binaural bands represent elements of subsystems that are largely segregated from each other at each level from the brainstem to at least the level of AI. Restricted injections of anterograde tracer into the central nucleus of the inferior colliculus (ICC) resulted in labeling of banded arrays in V (Andersen et al., 1980b). Those discontinuous patterns of label resemble the complex arrays that were labeled by intraband AI injections in this study. Restricted regions in the ICC receive their input from a limited number of the many brainstem nuclei that project to the colliculus (Roth et al., 1978; Semple and Aitkin, 1979). Together with the current observation of segregation of functionally distinguishable thalamocortical projections, these observations suggest that the inputs to different binaural bands in AI arise from different brainstem nuclei and ascend *in parallel* through the midbrain and thalamic levels to terminate in discrete bands in AI.

Segregation of ascending projections in auditory and visual systems. The intrinsic functional organization that we have observed in the auditory thalamus and cortex is analogous to some features of the functional organization of the visual system. In the auditory system, binaural bands apparently are the targets of parallel projections that arise in different brainstem nuclei and are isolated from each other at several subcortical levels. In the visual system, projections from the two retinae are segregated within discrete laminae in the lateral geniculate nucleus (LGN), and the LGN laminae project to eye-specific ocular dominance columns in the primary visual cortex (see Hubel and Wiesel, 1977). In the LGN, each lamina contains a representation of most of the retina. Similarly, EE- and EI-projecting regions in V each appear to extend across isofrequency laminae to encompass the representation of all of at least the basal half of the cochlea. Within AI, it appears that a single binaural band can contain a largely complete representation of the basal cochlea. This is not the case for ocular dominance columns, but this difference might simply reflect the difference between the one- and two-dimensional sensory epithelia of the auditory and visual systems.

Some functional implications. A systematic segregation of different classes of binaural neurons in AI and in their sources of input within V has been described in this report. What might be the functional significance of the complex intrinsic organization of this thalamocortical system?

Although we noted some quantitative differences between the responses of different EI units, at a superficial level of analysis there was no indication that the EI class could be subdivided. Conversely, differences in binaural responses within the EE class have been reported and, to some extent, associated with different binaural bands (Imig and Adrian, 1977; Merzenich et al., 1979; this study). Consistent with those physiological observations, different EI bands have been found in this study to derive their input from apparently coincident thalamic populations, but different EE bands derive input preferentially from different regions of a continuous EE-projecting zone.

If all EI bands apparently derive input from the same complex thalamic projection array and display, qualitatively, indistinguishable response properties in AI, what is indicated by the presence of multiple discrete EI bands? Perhaps the true functional unit is an *EI-EE band pair.* In general, responses of EI neurons are implicated in the neural representation of higher frequency sounds. It is now evident that AI integrity is essential for the localization of brief sounds (Jenkins and Merzenich, 1981) which, at higher frequencies, almost undoubtedly are encoded by EI neuronal populations. Also, recent studies (Middlebrooks and Pettigrew, 1981) have indicated that EI neurons in AI are sensitive to the location of a sound relative to the position of the cat's mobile external ear. Conversely, most nonspatial aspects of sound analysis probably are carried out within EE systems. One might hypothesize, then, that the EI bands confer information related to sound location upon the products of each of several response-specific EE zones.

In the lower frequency sector of AI, EE and EI bands have not been found, and there, small injections of retrograde tracer result in labeling of very continuous neuronal arrays in V (Colwell, 1977; Colwell and Merzenich, 1975, 1982). What might be the meaning of a banded projection in AI and the MGB that is present at the higher frequency aspects and lacking at lower frequen-

cies? One hypothesis might be that over the lower frequency range, binaural sound location and spectral information are processed within the *same* projection axis, while at higher frequencies they are processed within *different* subsystems. This is consistent with the hypothesis that at lower frequencies, both location and spectral information are encoded in temporal cues, while at higher frequencies, spectral analysis probably depends more on place coding and location sensitivity on intensive cues. In fact, it has been contended that sound spectrum decoding occurs largely within the line of projection of the medial superior olive (see Merzenich, 1981; Loeb et al., 1981), which is the principal nucleus implicated in the brainstem representation of the location of low frequency sounds. We hypothesize that within the representation of low frequencies, sound location representation is embedded within the same system that accounts for analysis of other features of sound, while a double (EE/EI) projection system applies for the higher frequency domain.

Binaural response-specific subdivisions as "cortical fields." It has been hypothesized that EI bands might interact closely with EE bands to confer sound location information on other aspects of sound feature extraction. It also is possible that EE and EI band classes each constitute discrete "representations." That is, individual bands or classes of bands could be operating largely independently of each other at or beyond AI in largely separate, parallel systems. Indeed, by the Rose and Woolsey criteria (Rose, 1949; Rose and Woolsey, 1949), it could be argued that the binaural band classes of "AI" each constitute a separate cortical field. As EE and EI subdivisions in the cat differ strikingly in their transcallosal projections (originating from large pyramidal cells in layer 3; Imig and Brugge, 1978), they presumably are delimitable cytoarchitecturally. Although there has been no clear description of cytoarchitectonic boundaries within AI in the cat, structural subdivisions have been observed within the presumptive primary fields in man and other primates (Economo, 1927; Bonin and Bailey, 1947; Bailey and Bonin, 1951; Pandya and Sanides, 1973). There, the auditory granular cortex contains "bands and islets" of cortex that are distinguished by the presence of larger layer 3 pyramidal cells. The two other Rose and Woolsey criteria, field-specific functional characteristics and field-specific differences in connectivity, also are met by the binaural band subdivisions of AI. In fact, the binaural *bands* of AI are as distinguishable by these criteria as are the various identified cochleotopic *fields* of the auditory area in the cat.

A further question. The current results demonstrate a large degree of convergence and divergence within the thalamic projection to AI. Projections from three elongated columns of cells in V converge onto restricted loci in single EI bands in AI. Similarly, the entire extent of a lamina in the rostral part of Vl converges onto single loci in EE bands, and single loci in this lamina diverge to three EE bands. The significance of this convergent and divergent organization remains a central question in understanding this complex projection system.

References

Adams, J. (1980) Stabilizing and rapid thionin staining of TMB-based HRP reaction product. Neurosci. Lett. *17:* 7–9.

Aitkin, L. M., and W. R. Webster (1972) Medial geniculate body of the cat: Organization and responses to tonal stimuli of neurons in the ventral division. J. Neurophysiol. *35:* 365–380.

Andersen, R. A. (1979) Patterns of connectivity of the auditory forebrain of the cat. Doctoral dissertation, University of California, San Francisco.

Andersen, R. A., P. L. Knight, and M. M. Merzenich (1980a) The thalamocortical and corticothalamic connections of AI, AII, and the anterior auditory field (AAF) in the cat: Evidence for two largely segregated systems of connections. J. Comp. Neurol. *194:* 663–701.

Andersen, R. A., G. L. Roth, L. M. Aitkin, and M. M. Merzenich (1980b) The efferent projections of the central nucleus and the pericentral nucleus of the inferior colliculus in the cat. J. Comp. Neurol. *194:* 649–662.

Bailey, P., and G. von Bonin (1951) The isocortex of man. In *Illinois Monographs in the Medical Sciences*, R. M. Allen, O. F. Kampmeier, I. Schour, and E. R. Serles, eds., Vol. 6, pp. 1–301, University of Illinois Press, Urbana, IL.

Bentivoglio, M., H. G. J. M. Kuypers, and C. E. Catsman-Berrevoets (1980a) Retrograde neuronal labeling by means of bisbenzimide and Nuclear Yellow (Hoechst S769121). Measures to prevent diffusion of the tracers out of retrogradely labeled neurons. Neurosci. Lett. *18:* 19–24.

Bentivoglio, M., H. G. J. M. Kypers, C. E. Catsman-Berrevoets, H. Loewe, and O. Dann (1980b) Two new fluorescent retrograde neuronal tracers which are transported over long distances. Neurosci. Lett. *18:* 25–30.

Bonin, G. von, and P. Bailey (1947) The neocortex of *Macaca mulatta*. In *Illinois Monographs in the Medical Sciences*, R. M. Allen, O. F. Kampmeier, I. Schour, and E. R. Serles, eds., Vol. 5, pp. 1–163, University of Illinois Press, Urbana, IL.

Calford, M. B., and W. R. Webster (1981) Auditory representation within principal division of cat medial geniculate body: An electrophysiological study. J. Neurophysiol. *45:* 1013–1028.

Colwell, S. A. (1977) Corticothalamic projections from physiologically defined loci within primary auditory cortex in the cat: Reciprocal structure in the medial geniculate body. Doctoral dissertation, University of California, San Francisco.

Colwell, S. A., and M. M. Merzenich (1975) Organization of thalamocortical and corticothalamic projections to and from physiologically defined loci within primary auditory cortex in the cat. Anat. Rec. *181:* 336.

Colwell, S. A., and M. M. Merzenich (1982) Corticothalamic projections from physiologically defined loci in AI in the cat. J. Comp. Neurol., in press.

deRibaupierre, F., A. Toros, and Y. deRibaupierre (1975) Acoustical responses of single units in the medial geniculate body of the cat. Exp. Brain Res. (Suppl.) *23:* S98.

Economo, C. von (1927) *L'Architecture Cellulaire Normale de L'Ecorce Cerebral.* Masson, Paris.

Evans, E. F., H. F. Ross, and I. C. Whitfield (1965) The spatial distribution of unit characteristic frequency in the primary auditory cortex of the cat. J. Physiol. (Lond.) *177:* 238–247.

Goldstein, M. H., Jr., M. Abeles, R. L. Daly, and J. McIntosh (1970) Functional architecture in cat primary auditory cortex: Tonotopic organization. J. Neurophysiol. *33:* 188–197.

Hubel, D. H., and T. N. Wiesel (1977) Functional architecture of macaque monkey visual cortex. Proc. R. Soc. Lond. (Biol.) *198:* 1–59.

Imig, T. J., and H. O. Adrian (1977) Binaural columns in the primary field (AI) of cat auditory cortex. Brain Res. *138:* 241–257.

Imig, T. J., and J. F. Brugge (1978) Sources and terminations of callosal axons related to binaural and frequency maps in primary auditory cortex of the cat. J. Comp. Neurol. *182:* 637–660.

Imig, T. J., and R. A. Reale (1981) Ipsilateral corticocortical

projections related to binaural columns in cat primary auditory cortex. J. Comp. Neurol. *203:* 1-14.

Jenkins, W. M., and M. M. Merzenich (1981) Lesions of restricted representation sectors within primary auditory cortex produce frequency dependent sound localization deficits. Soc. Neurosci. Abstr. *7:* 392.

Jones, E. G., and T. P. S. Powell (1971) An analysis of the posterior group of thalamic nuclei on the basis of its afferent connections. J. Comp. Neurol. *143:* 185-216.

Kitzes, L. M., K. S. Wrege, and J. M. Casseday (1980) Patterns of responses of cortical cells to binaural stimulation. J. Comp. Neurol. *192:* 455-472.

Kuypers, H. G. J. M., M. Bentivoglio, D. van der Kooy, and C. E. Catsman-Berrevoets (1979) Retrograde transport of bisbenzimide and propidium iodide through axons to their parent cell bodies. Neurosci. Lett. *12:* 1-7.

Loeb, G. E., M. W. White, and M. M. Merzenich (1981) Mechanisms of auditory information processing for pitch perception. Soc. Neurosci. Abstr. *7:* 56.

Merzenich, M. M. (1981) Some recent observations on the functional organization of the central auditory nervous system. In *Brain Mechanisms of Sensation,* Y. Katsuki, R. Norgren, and M. Sato, eds., John Wiley & Sons, New York.

Merzenich, M. M., P. L. Knight, and G. L. Roth (1975) Representation of the cochlea within the primary auditory cortex in the cat. J. Neurophysiol. *38:* 231-249.

Merzenich, M. M., R. A. Andersen, and J. C. Middlebrooks (1979) Functional and topographic organization of the auditory cortex. Exp. Brain Res. (Suppl.) *2:* 61-75.

Merzenich, M. M., S. A. Colwell, and R. A. Andersen (1982) Thalamocortical and corticothalamic connections in the auditory system of the cat. In *Cortical Sensory Organization III,* C. N. Woolsey, ed., pp. 43-57, Humana Press, Clifton, NJ.

Mesulam, M. -M. (1978) Tetramethyl benzidine for horseradish peroxidase neurohistochemistry. A non-carcinogenic blue reaction-product with superior sensitivity for visualizing neural afferents and efferents. J. Histochem. Cytochem. *26:* 106-117.

Middlebrooks, J. C. (1982) Subunits of the primary auditory cortex (AI) of the cat distinguished by segregated thalamic input sources and functional specialization. Doctoral dissertation, University of California, San Francisco.

Middlebrooks, J. C., and J. D. Pettigrew (1981) Functional classes of neurons in primary auditory cortex of the cat distinguished by sensitivity to sound location. J. Neurosci. *1:* 107-120.

Middlebrooks, J. C., and J. M. Zook (1981) Thalamic connections to and from binaural interaction bands in AI of the cat. Soc. Neurosci. Abstr. *7:* 230.

Middlebrooks, J. C., R. W. Dykes, and M. M. Merzenich (1980) Binaural response-specific bands in primary auditory cortex (AI) of the cat: Topographical organization orthogonal to isofrequency contours. Brain Res. *181:* 31-48.

Moore, R. Y., and J. M. Goldberg (1963) Ascending projections of the inferior colliculus in the cat. J. Comp. Neurol. *121:* 109-135.

Morest, D. K. (1964) The neuronal architecture of the medial geniculate body of the cat. J. Anat. *98:* 611-680.

Morest, D. K. (1965) The laminar structure of the medial geniculate body of the cat. J. Anat. *99:* 143-160.

Neff, W. D., J. F. Fisher, I. T. Diamond, and M. Yela (1956) Role of auditory cortex in discrimination requiring localization of sound in space. J. Neurophysiol. *19:* 500-512.

Niimi, K., and H. Matsuoka (1979) Thalamocortical organization of the auditory system in the cat studied by retrograde axonal transport of horseradish peroxidase. Adv. Anat. Embryol. Cell Biol. *57:* 1-54.

O'Neill, W. E., and N. Suga (1982) Encoding of target range and its representation in the auditory cortex of the mustached bat. J. Neurosci. *2:* 17-31.

Oonishi, S., and Y. Katsuki (1965) Functional organization and integrative mechanism in the auditory cortex of the cat. Jpn. J. Physiol. *15:* 342-365.

Pandya, D. M., and F. Sanides (1973) Architectonic parcellation of the temporal operculum in Rhesus monkey and its projection pattern. Z. Anat. Entwicklungs-gesch. *139:* 127-161.

Phillips, D. P., and D. R. F. Irvine (1981) Responses of single neurons in physiologically defined area AI of cat cerebral cortex: Sensitivity to interaural intensity differences. Hear. Res. *4:* 299-307.

Reale, R. A., and T. J. Imig (1980) Tonotopic organization in auditory cortex of the cat. J. Comp. Neurol. *192:* 265-292.

Rose, J. E. (1949) The cellular structure of the auditory region of the cat. J. Comp. Neurol. *91:* 409-440.

Rose, J. E., and C. N. Woolsey (1949) The relations of thalamic connections, cellular structure, and evocable activity in the auditory region of the cat. J. Comp. Neurol. *91:* 441-466.

Roth, G. L., L. M. Aitkin, R. A. Andersen, and M. M. Merzenich (1978) Some features of the spatial organization of the central nucleus of the inferior colliculus of the cat. J. Comp. Neurol. *182:* 661-680.

Semple, M. N., and L. M. Aitkin (1979) Representation of sound frequency and laterality by units in central nucleus of cat inferior colliculus. J. Neurophysiol. *42:* 1626-1639.

Sousa-Pinto, A. (1973) The structure of the first auditory cortex (AI) in the cat. I. Light microscopic observations on its organization. Arch. Ital. Biol. *111:* 112-137.

Suga, N., and W. E. O'Neill (1980) Auditory processing of echos: Representation of acoustic information from the environment in the bat cerebral cortex. In *Animal Sonar Systems,* R. -G. Busnel and J. F. Fish, eds., pp. 589-611, Plenum Press, New York.

Toros, A., E. Rouiller, Y. deRibaupierre, C. Ivarsson, M. Holden, and F. deRibaupierre (1979) Changes of functional properties of medial geniculate body neurons along the rostrocaudal axis. Neurosci. Lett. (Suppl.) *3:* S5.

Tunturi, A. R. (1950) Physiological determination of the arrangement of the afferent connections to the middle ectosylvian auditory area in the dog. Am. J. Physiol. *162:* 489-502.

Tunturi, A. R. (1952) A difference in the representation of auditory signals from the left and right ears in the isofrequency contours of the right middle ectosylvian auditory cortex of the dog. Am. J. Physiol. *168:* 712-727.

Wilson, M. E., and B. G. Cragg (1969) Projection from the medial geniculate body to the cerebral cortex of the cat. Brain Res. *13:* 462-475.

Winer, J. A., I. T. Diamond, and D. Raczkowski (1977) Subdivision of the auditory cortex of the cat: The retrograde transport of horseradish peroxidase to the medial geniculate body and posterior thalamic nuclei. J. Comp. Neurol. *176:* 387-418.